Postprint of: Czyżniewski M., Łangowski R.: A robust sliding mode observer for non-linear uncertain biochemical systems, ISA TRANSACTIONS (2021), DOI: 10.1016/j.isatra.2021.05.040

A robust sliding mode observer for non-linear uncertain biochemical systems

Mateusz Czyżniewski[a], Rafał Łangowski[a,*]

[a]*Department of Electrical Engineering, Control Systems and Informatics, Gdańsk University of Technology, G. Narutowicza 11/12, 80-233 Gdańsk, Poland*

ARTICLE INFO

Keywords:
bioreactors
non-linear uncertain systems
observers
process modelling
state estimation

ABSTRACT

A problem of state estimation for a certain class of non-linear uncertain systems has been addressed in this paper. In particular, a sliding mode observer has been derived to produce robust and stable estimates of the state variables. The stability and robustness of the proposed sliding mode observer have been investigated under parametric and unstructured uncertainty in the system dynamics. In order to ensure an unambiguous non-linear state (coordinates) transformation, the appropriate system model for the observer synthesis has been devised and analysed. The stability analysis of dynamics of estimation error has been carried out, based on the Lyapunov stability theory in relation to Lipschitz assumptions for non-linear functions. In order to validate the performance of the devised observer, it has been applied to the model of a continuous stirred tank reactor (bioreactor). The promising simulation results have been obtained and they demonstrate the high effectiveness of the devised approach.

Principal symbols and abbreviations

CSTR	continuous stirred tank reactor
SMO	sliding mode observer
UIO	unknown input observer
Σ	class of non-linear affine systems
Σ_{c}	class of considered non-linear affine systems
Σ_{CSTR}	cognitive model of considered processes in a CSTR
$\Sigma^{\mathrm{OS}}_{\mathrm{CSTR}}$	utility model of considered processes in a CSTR
$\boldsymbol{A}$	constant matrix of the linear part of system dynamics
$\boldsymbol{b}(\boldsymbol{x}(t))$	smooth mapping associated with control inputs
β_{m}	biomass mortality rate
$\beta_{\tilde{\rho}}$	bounding constant of $\tilde{\boldsymbol{\rho}}(\cdot)$
$\beta_{\mathrm{u_r}}$	bounding constant of $u_{\mathrm{r}}(\cdot)$
$\boldsymbol{C}$	constant matrix of outputs
$D(t)$	bounded dilution rate
$\Delta(\boldsymbol{x}(t), t)$	unknown bounded input
$\boldsymbol{\varepsilon}(t)$	estimation error

*Corresponding author
rafal.langowski@pg.edu.pl (R. Łangowski)
ORCID(s): 0000-0003-1150-9753 (R. Łangowski)

$\tilde{\boldsymbol{\varepsilon}}(t)$	estimation error in the new coordinates
$\boldsymbol{f}(\boldsymbol{x}(t),t)$	smooth mapping associated with internal dynamics
$\hat{\boldsymbol{f}}(\boldsymbol{x}(t))$	exactly known component of $\boldsymbol{f}(\boldsymbol{x}(t),t)$
$\boldsymbol{\Phi}(\boldsymbol{x}(t))$	non-linear state transformation
$h(\boldsymbol{x}(t))$	smooth mapping associated with output
$K_{\mathrm{i}}(t)$	time–varying coefficient of the reaction inhibition
$K_{\mathrm{s}}(t)$	time–varying coefficient of saturation
$\boldsymbol{K}^{\mathrm{SMO}}$	gains vector of proportional part of SMO
L^{SMO}	gain of sliding part of SMO
$L^{(\cdot)}_{(\cdot)}(\cdot)$	Lie derivative
$L_{(\cdot)}$	Lipschitz constant
$\lambda_{\max}(\cdot)$	maximal eigenvalue
m_{s}	substrate concentration maintenance coefficient
$\mu_{\mathrm{H}}(t)$	Haldane kinetics function
$\mu^{[1]}_{\mathrm{M}}(S(t),t)$	Monod kinetics function
$\hat{\mu}_{\mathrm{M}}(t)$	simplified Monod kinetics function
$\mu_{\max}(t)$	time–varying maximum growth rate parameter
$\mu_0(t)$	substitute coefficient of the kinetics reaction
Ω	set of all possible system states
$\tilde{\boldsymbol{\psi}}(\tilde{\boldsymbol{x}}(t),u(t))$	non-linear mapping
$r(t)$	growth rate function
$\boldsymbol{\rho}(\boldsymbol{x}(t))$	vector parameterising the uncertainties
$\tilde{\boldsymbol{\rho}}(\tilde{\boldsymbol{x}}(t))$	non-linear mapping
$S(t)$	concentration of aggregated substrate
S_{in}	concentration of substrate in inflow to a CSTR
t	time instant
$u(t)$	bounded control input
$X(t)$	concentration of aggregated biomass
$\boldsymbol{x}(t)$	vector of state variables
$\tilde{\boldsymbol{x}}(t)$	vector of state variables in the new coordinates
$\hat{\boldsymbol{x}}(t)$	vector of estimated state variables
$\hat{\tilde{\boldsymbol{x}}}(t)$	vector of estimated state variables in the new coordinates
$\boldsymbol{V}_{(\cdot)}(\cdot)$	Lyapunov function
Y	substrate growth yield coefficient
$y(t)$	measurable output

1. Introduction

The modern control theory distinguishes two widely used terms, i.e. control systems and monitoring systems. Undoubtedly, they involve the problem of accessing information about the process variables (the current state, controlled outputs, etc.) of a given process. This information is provided by the measuring devices (sensors) installed in the plant where the process takes place. Unfortunately, not all process variables are physically measurable or it is not possible to allocate the necessary number of sensors, e.g., [1–3]. It is due to, e.g., a lack of suitable measuring devices or their high costs, and physical capacity for their installation. Therefore, the missing information about, e.g., the state variables needs to be recovered by employing their estimates. Typically, the estimation process is based on measurements of other available variables and the mathematical model of the process. In general, the accuracy (performance) of the estimation process depends on the nature of the considered process, the accuracy of the model used for estimation purposes, and the quality of the used (primarily measuring) data, e.g., [4, 5].

In the literature a large number of publications devoted to both the state and parameter estimation as well as joint estimation (state and parameter) can be found. For instance, from the pioneering work of Luenberger and Kalman, which provided linear state observers generating point estimates for deterministic systems and with probabilistically modelled uncertainty [5, 6] respectively, through different kinds of interval observers, e.g., [7–10], and non-linear observers, e.g., [3, 4, 11–15]. This work focuses on one of the varieties of non-linear observers, namely sliding mode observers (SMOs). In general, the sliding mode observers enable effective estimation of the state of uncertain dynamic systems. It is well–known that the mathematical (cognitive) model is only the end of an accurate representation of reality. Clearly, the unstructured and parametric (structured) uncertainty may be appeared. The unstructured uncertainty usually stems from an unmodelled dynamics (includes model simplifications) whereas the parametric uncertainty holds inaccurate knowledge of the values of given parameters. The SMOs are able to handle the parametric and unstructured uncertainties in the system dynamics (also disturbances) by using the ideas of sliding surfaces and the equivalent control [13, 16–22]. Hence, they are able to generate the robust estimates of the state variables. In the literature there are several kinds of SMO structures, but typically they are based on treating uncertainty as a kind of observer unknown input. Hence, SMOs may be considered also as unknown input observer (UIO) [13, 16, 19, 23–25]. Moreover, the SMOs have found many applications in the areas such as electromechanical systems, e.g., [21, 26], fault detection and diagnosis, e.g., [18, 27–30] and state estimation in chemical and biochemical processes, e.g., [13, 31–36].

As it has been mentioned above, a proper mathematical model of the considered process is necessary for estimation purposes. Unfortunately, there are many situations when the cognitive model cannot be used as a utility model for estimation purposes due to time–varying parameters, unknown external inputs, and above–mentioned unstructured uncertainty, e.g., [13, 19, 37, 38]. Therefore, one of the main problems during observer synthesis is to derive a simpler substitute model of the considered process (system). It is obvious that simplification of the cognitive model can notably influence the accuracy of the representation of reality, and become another source of unstructured uncertainty. Hence, the preparation of the model for observer synthesis purposes is always associated with a reduction of the level of mathematical complexity. Therefore, it is always needed to provide a kind of trade–off between accuracy and simplicity of the model. Moreover, the certain important aspects associated with model observability and detectability should be taken into account. Clearly, the considered model may be unobservable due to, e.g., unknown inputs occurrence or non-injectivity of the coordinate transformation [24]. Thus, the proper modifications of the utility model can be needed to ensure the state observability.

In this work, due to the background of the problem, the SMO structure introduced in [13, 25, 36, 39, 40] is used and further developed. This structure integrating a high-gain approach, e.g., [12, 41] with a sliding mode approach to the estimation of the state variables. Hence, the main aim of this work is to deliver a robust observer for the state estimation purposes of a certain class of non-linear affine systems. Thus, the essential aspects associated with models reconstruction are presented. For instance, a large number of chemical and biochemical processes belong to this class, a continuous stirred tank reactor (CSTR) (bioreactor) with the microbial growth reaction and their mortality with the aggregated substrate and biomass (reactants) concentrations [37] is considered in this paper, in particular. Moreover, in comparison to the methodology presented in [13, 25, 36, 39, 40], authors devised the sliding mode observer which rejects not only the negative impact of the disturbances or the components of dynamics which parameters are time–variant (e.g. uncertain kinetics of biochemical processes), but also deal with unstructured uncertainty. Thus, the main contributions of this paper are as follows:

a) the sliding mode observer producing stable and robust estimates of the state variables despite the parametric and unstructured uncertainty in the system dynamics has been devised,

b) the proper utility model for sliding mode observer design purposes has been developed and its main features have been investigated,

c) the comprehensive analysis of the impact of observer gain matrix values on eigenvalues of the Lyapunov matrix has been given.

The paper is organised as follows. The problem formulation is presented in section 2. Section 3 includes the derivation of the cognitive model of considered processes. The fundamental information about sliding mode observers is given in section 4. Section 5 includes the derivation of the utility model for estimation purposes. The synthesis of the sliding mode observer for bioreactor is given in section 6. The simulation results are described in section 7. The paper is concluded in section 8 and completed with three appendices.

2. Problem statement

Considering $\mathbb{R}^{\mathrm{n}}$ as the n–dimensional vector space over a real number field $\mathbb{R}$, a certain class of non-linear affine systems Σ can be defined as follows [42, 43]:

$$\Sigma : \begin{cases} \dot{\boldsymbol{x}}(t) & = \boldsymbol{f}\left(\boldsymbol{x}(t), t\right) + \boldsymbol{b}\left(\boldsymbol{x}(t), t\right) u(t) + \boldsymbol{w}\left(\boldsymbol{x}(t), t\right) \boldsymbol{z}(t) \\ \boldsymbol{x}(t_0) & = \boldsymbol{x}_0 \\ y(t) & = h\left(\boldsymbol{x}(t), u(t), \boldsymbol{v}(t), t\right) \end{cases}, \tag{1}$$

where: $\dot{(\cdot)}$ stands for the derivative with respect to t; $t \in \mathbb{T} = \mathbb{R}_+ \cup \{0\} \subset \mathbb{R}$ is the time instant, $\mathbb{R}_+$ denotes a positive part of $\mathbb{R}$; $\forall t \in \mathbb{T}: \ \boldsymbol{x}(t) \in \mathbb{X}_{\mathrm{n}} \subset \mathbb{R}^{\mathrm{n}}$ is the vector of state variables, which coincide with globally defined cubic coordinates, $\mathbb{X}_{\mathrm{n}}$ is a (connected) differentiable manifold with a $C^{\infty}(\cdot)$ structure of dimension n; $\forall t \in \mathbb{T}: \ u(t) \in \mathbb{U} \subset \mathbb{R}$, $|u(t)| \leq u_{\mathrm{bound}} < \infty$ denotes the bounded by u_{bound} control input, and $|\cdot|$ is an absolute value of $(\cdot)$; $\forall t \in \mathbb{T}: \ \boldsymbol{z}(t) \in \mathbb{Z}_{\mathrm{m}} \subset \mathbb{R}^{\mathrm{m}}$, $||\boldsymbol{z}(t)||_{\infty} = \max\left\{\sup\left\{\left|z_{i_{\mathrm{m}}}\right| : \ t \in \mathbb{T}\right\}, i_{\mathrm{m}} = \overline{1, m}\right\} \leq z_{\mathrm{bound}} < \infty$ signifies the bounded by z_{bound} vector of disturbance inputs, and $||\cdot||$ denotes an infinity norm of $(\cdot)$, $\max\{\cdot\}$ is a maximum of $(\cdot)$, and $\sup\{\cdot\}$ denotes a supremum of $(\cdot)$; $\forall t \in \mathbb{T}: \ y(t) \in \mathbb{Y} \subset \mathbb{R}$ is the measurable output; $\forall t \in \mathbb{T}: \ \boldsymbol{v}(t) \in \mathbb{V}_{\mathrm{l}} \subset \mathbb{R}^{\mathrm{l}}$ denotes the vector of measurement noise; $\forall t \in \mathbb{T}: \ \boldsymbol{f}: \ \mathbb{X}_{\mathrm{n}} \times \mathbb{T} \to T\mathbb{X}_{\mathrm{n}}$, $\forall t \in \mathbb{T}: \ \boldsymbol{b}, \boldsymbol{w}: \ \mathbb{X}_{\mathrm{n}} \times \mathbb{T} \to T\mathbb{X}_{\mathrm{n}}$, $\forall t \in \mathbb{T}: \ h: \ \mathbb{X}_{\mathrm{n}} \times \mathbb{U} \times \mathbb{V}_{\mathrm{l}} \times \mathbb{T} \to \mathbb{R}$ are smooth maps, and $\times$ denotes a Cartesian product; $T(\cdot)$ is the tangent bundle of vector field.

It should be added that the system Σ is claimed as complete, i.e. the state trajectories $\boldsymbol{x}(t)$ are defined for every $t \in \mathbb{T}$, every initial condition $\boldsymbol{x}_0$ and for all exogenous signals which belong to their particular sets.

The following features describe the frame of uncertainties and the minimum knowledge on the considered system Σ_{c} belonging to (1):

I. $\forall t \in \mathbb{T}: \ \boldsymbol{f}\left(\boldsymbol{x}(t), t\right)$ is not exactly known; clearly, $\forall t \in \mathbb{T}: \ \boldsymbol{f}\left(\boldsymbol{x}(t), t\right)$ is burden by parametric and unstructured uncertainty,

II. it is assumed that there is only bounded control input $u(t)$ in the considered system,

III. $\forall t \in \mathbb{T}: \ \boldsymbol{b}\left(\boldsymbol{x}(t), t\right)$ is known and time–invariant with respect to parameters, hence $\forall t \in \mathbb{T}: \ \boldsymbol{b}: \ \mathbb{X}_{\mathrm{n}} \to T\mathbb{X}_{\mathrm{n}}$, $\forall t \in \mathbb{T}: \ \boldsymbol{b}\left(\boldsymbol{x}(t), t\right) \to \boldsymbol{b}\left(\boldsymbol{x}(t)\right)$,

IV. due to system dynamics the measurement noise can be neglected, therefore $\forall t \in \mathbb{T}: \ h\left(\boldsymbol{x}(t), u(t), \boldsymbol{v}(t), t\right) \to h\left(\boldsymbol{x}(t), u(t), t\right)$,

V. $\forall t \in \mathbb{T}: \ h\left(\boldsymbol{x}(t), u(t), t\right)$ is time–invariant with respect to parameters and control input, thus $\forall t \in \mathbb{T}: \ h: \ \mathbb{X}_{\mathrm{n}} \to \mathbb{Y}$, $\forall t \in \mathbb{T}: \ h\left(\boldsymbol{x}(t), u(t), t\right) \to h\left(\boldsymbol{x}(t)\right)$.

Hence, including I–V, the Σ_{c} yields:

$$\Sigma_{\mathrm{c}} : \begin{cases} \dot{\boldsymbol{x}}(t) & = \hat{\boldsymbol{f}}(\boldsymbol{x}(t)) + \boldsymbol{b}(\boldsymbol{x}(t))u(t) + \boldsymbol{\rho}(\boldsymbol{x}(t))\Delta(\boldsymbol{x}(t), t) \\ \boldsymbol{x}(t_0) & = \boldsymbol{x}_0 \\ y(t) & = h(\boldsymbol{x}(t)) \end{cases}, \tag{2}$$

where $\forall t \in \mathbb{T}: \ \hat{\boldsymbol{f}}: \ \mathbb{X}_{\mathrm{n}} \rightarrow T\mathbb{X}_{\mathrm{n}}$ stands for an exactly known component of $\boldsymbol{f}(\cdot)$ resulting from the elimination of parametric and unstructured uncertainty, and their modelling as:

$$\boldsymbol{\rho}(\boldsymbol{x}(t))\Delta(\boldsymbol{x}(t),t) \triangleq \boldsymbol{f}(\boldsymbol{x}(t),t) - \hat{\boldsymbol{f}}(\boldsymbol{x}(t)), \tag{3}$$

where $\forall t \in \mathbb{T}: \ \boldsymbol{\rho}: \ \mathbb{X}_{\mathrm{n}} \rightarrow T\mathbb{X}_{\mathrm{n}}$ is the vector parameterising the uncertainties and $\forall t \in \mathbb{T}: \ \Delta: \ \mathbb{X}_{\mathrm{n}} \times \mathbb{T} \rightarrow \mathbb{R}$ with $||\Delta(\boldsymbol{x}(t),t)||_{\infty} = \max\left\{|\Delta(\boldsymbol{x}(t),t)| : \ (\boldsymbol{x},t) \in \mathbb{X}_{\mathrm{n}} \times \mathbb{T}\right\} \leq \overline{\Delta} < \infty$. It is worth noting that $\Delta(\boldsymbol{x}(t),t)$ may be considered as an unknown bounded by $\overline{\Delta}$ input to the considered system Σ_{c}. In fact, the $\Delta(\boldsymbol{x}(t),t)$ component must be imposed in every of the state equations of considered system [13, 25, 39]. This claim provide the opportunity to perform compensation of the uncertainty for the whole system dynamics.

In order to simplify notation the following definitions are introduced:

- $\boldsymbol{x}(t) \triangleq \boldsymbol{x}(t, \boldsymbol{x}_0, u(t), \Delta(\boldsymbol{x}(t),t))$ is a general solution of system Σ_{c} related to $\boldsymbol{x}_0$, $u(t)$ and $\Delta(\boldsymbol{x}(t),t)$,
- $y(t) \triangleq y(\boldsymbol{x}(t, \boldsymbol{x}_0, u(t), \Delta(\boldsymbol{x}(t),t))) = h(\boldsymbol{x}(t, \boldsymbol{x}_0, u(t), \Delta(\boldsymbol{x}(t),t)))$ is the output functional related to $\boldsymbol{x}_0$, $u(t)$ and $\Delta(\boldsymbol{x}(t),t)$.

As it has been mentioned above, this work aims to deliver a robust observer for the state estimation purposes of non-linear systems type Σ_{c}. Because a large number of chemical and biochemical processes can be described by (2), a CSTR with the microbial growth reaction and their mortality with the aggregated substrate and biomass concentrations [37] is considered in the further part of the paper. It is worth adding that the proposed methodology may be applied to more complex systems based on a CSTR, e.g., bioreactor with the settler. Moreover, the idea of simplifying the kinetics function can be utilised in the context of multi-variable, where more than one substrate appears in dynamics.

3. Cognitive model of the considered system

A CSTR with the microbial growth reaction and their mortality with the aggregated substrate $S(t) \ \left[g/L\right]$ and biomass $X(t) \ \left[g/L\right]$ concentrations is one of the most widely used biochemical processes models [37]:

$$S(t) \rightarrow X(t). \tag{4}$$

For further considerations the set of all possible system states is defined as:

$$\Omega = \{(X(t), S(t)) \in \mathbb{R}^2: \ \forall t \in \mathbb{T}: \ 0 \leq X(t) \leq \overline{X}, \ 0 \leq S(t) \leq \overline{S}\}, \tag{5}$$

where $\overline{X}$ and $\overline{S}$ are (real) the upper bounds of the particular reactant. It is worth adding that Ω is an invariant set meeting the condition of the general theory of biochemical processes dynamics [10, 37]: $\Omega \subset \mathbb{X}_{\mathrm{n}} \subset \mathbb{R}^2$.

The dynamics of the considered model is described by the following phenomena [37]:

a) the microbial growth reaction (reaction kinetics) in the CSTR is described by growth rate function, $r(t) \geq 0 \left[g/hL\right]$,

b) the inflow and outflow in the CSTR are described by the bounded dilution rate, $0 \leq D(t) \leq \overline{D} \left[h^{-1}\right]$,

c) the microbial mortality is taken into account in the CSTR dynamics in the following way:

$$\begin{aligned} \text{biomass death: } & X(t) \rightarrow X_{\mathrm{d}}(t), \\ \text{substrate maintenance: } & S(t) + X(t) \rightarrow X(t), \end{aligned}$$

where $X_{\mathrm{d}} \left[g/L\right]$ is the dead biomass.

From the constituent mass balance law, the model of considered processes in the CSTR Σ_{CSTR}, taking into account the above–mentioned phenomena, can be written as follows [37]:

$$\Sigma_{\mathrm{CSTR}}: \begin{cases} \dot{X}(t) & = r(t) - \beta_{\mathrm{m}} X(t) - X(t)D(t) \\ \dot{S}(t) & = -\dfrac{1}{Y} r(t) - m_{\mathrm{s}} X(t) + (S_{\mathrm{in}} - S(t))D(t) \\ X(t_0) & = X_0 \\ S(t_0) & = S_0 \end{cases}, \tag{6}$$

where: $\forall t \in \mathbb{T}: \ Y > 0\,[-]$, $S_{\text{in}} > 0\,\left[g/L\right]$, $\beta_{\text{m}} > 0\,\left[h^{-1}\right]$, $m_{\text{s}} > 0\,\left[h^{-1}\right]$ denote the yield coefficient of substrate growth, substrate concentration in inflow to the CSTR, biomass mortality rate, and coefficient of substrate concentration maintenance, respectively. This particular system may be considered as an epitome example of the biochemical reaction system, which present the most important structural properties of the whole class of systems [37].

One of the most important parts of the dynamics of biochemical processes is the reaction kinetics, which is also one of the uncertainty sources. In general, this function is claimed as a very uncertain, complex and time–varying component of the model [9, 10, 37, 44–49]. In fact, the kinetics of the reactions are affected by the biological components concentrations occurring in the bioreactors. Typically, they are represented by non-linear, non-negative, and uncertain functions referring to the particular concentrations of reactants in the liquid phase [37, 44]. A widespread approach to formulating their models is given by the following law:

$$r(t) = \prod_{i_{\text{c}}=1}^{n_{\text{c}}} \mu_{(\cdot)}^{[i_{\text{c}}]}(\cdot, t), \tag{7}$$

where $\forall t \in \mathbb{T}: \ \mu_{(\cdot)}^{[i_{\text{c}}]}(\cdot, t)\,\left[g/hL\right]$ and n_{c} denote specific growth rate which separately represents the effect of each component of the rate and number of reactants involved in a reaction, respectively. The lower index of $\mu_{(\cdot)}^{[i_{\text{c}}]}(\cdot, t)$ denotes the kind of structure of the considered specific growth rate and the upper index refers to particular reactant concentration.

It is crucial to state that model of every specific growth rate should properly represent the physical phenomenon. Therefore, the growth rate satisfies the following conditions [9, 10, 37, 44–48]:

1) $r(t) = 0$, when one of the state dependent arguments of the particular $\mu_{(\cdot)}^{[\cdot]}(\cdot, t)$ is equal to zero,

2) $\forall t \in \mathbb{T}: \ r(t)$ is positive and bounded only when its all of the state dependent arguments are positive,

3) $r(t)$ is always continuous function of its parameters and states of a system.

A large number of possible models to express the $\mu_{(\cdot)}^{[\cdot]}(\cdot, t)$ can be found in the literature, e.g., [48]. Among the most common models are: Linear, Monod and Haldane functions, denoted by $\mu_{\text{L}}^{[\cdot]}(\cdot, t)$, $\mu_{\text{M}}^{[\cdot]}(\cdot, t)$ and $\mu_{\text{H}}^{[\cdot]}(\cdot, t)$, respectively. For instance the substrate concentration dependent Monod function based on Michaelis–Menten law is given by:

$$\mu_{\text{M}}^{[1]}(S(t), t) = \mu_{\max}(t)\frac{S(t)}{K_{\text{s}}(t) + S(t)}, \tag{8}$$

where $\forall t \in \mathbb{T}: \ \mu_{\max}(t) > 0 \in \mathbb{R}_{+}\,\left[h^{-1}\right]$ is the time–varying maximum growth rate parameter and $\forall t \in \mathbb{T}: \ K_{\text{s}}(t) \in \mathbb{R}_{+}\,\left[g/L\right]$ denotes the time–varying coefficient of saturation. It is worth mentioning that Monod function and its derivative $\forall t \in \mathbb{T}: \ \dot{\mu}_{\text{M}}^{[\cdot]}(\cdot, t) > 0$ are monotonic functions of their argument.

In turn, the Haldane function is as follows:

$$\begin{aligned} \mu_{\text{H}}^{[1]}(S(t), t) &= \mu_0(t)\frac{S(t)}{K_{\text{s}}(t) + S(t) + \dfrac{S^2(t)}{K_{\text{i}}(t)}}, \\ \mu_0(t) &= \mu_{\max}(t)\left(1 + 2\sqrt{\frac{K_{\text{s}}(t)}{K_{\text{i}}(t)}}\right), \end{aligned} \tag{9}$$

where $\forall t \in \mathbb{T}: \ \mu_0(t) \in \mathbb{R}_{+}\,\left[h^{-1}\right]$ is the substitute coefficient of the kinetics reaction and $\forall t \in \mathbb{T}: \ K_{\text{i}}(t) \in \mathbb{R}_{+}\,\left[g/L\right]$ denotes the time–varying coefficient of the reaction inhibition.

It should be noted that it is commonly assumed that structure of reaction kinetics model is known (e.g. presented models of the Monod or Haldane) whereas the parameters $\left(\mu_{\max}(t), K_{\text{s}}(t), K_{\text{i}}(t)\right)$ are claimed as uncertain. This issue occurs in many biochemical applications because:

i) a lack of sufficient knowledge about the calibrated values of model parameters,

ii) the need for simplification of the model structure concerning the process complexity or conditions for particular algorithm synthesis.

Hence, in the CSTR model (6) reaction rate which models transformation of the substrate $S(t)$ to the biomass $X(t)$ is modelled by using formula (7) as [9, 37, 44, 45]:

$$r(t) \triangleq \mu^{[1]}_{(\cdot)}(S(t),t)\mu^{[2]}_{\mathrm{L}}(X(t)) = \mu^{[1]}_{(\cdot)}(S(t),t)X(t). \tag{10}$$

In this work, the reaction rate is modelled as the product of the Haldane function (9) and the Linear function of biomass, therefore the formula (10) is using in (6). Henceforth, due to occurrence of only one kinetics function in (6), to provide simplified indication of the particular kinetics functions, the upper index and state dependent arguments have been omitted what has been denoted as: $\mu^{[1]}_{\mathrm{H}}(S(t),t) \rightarrow \mu_{\mathrm{H}}(t)$. In turn, because of necessity of modelling the kinetics function parameters uncertainty, the following approach is proposed:

$$\begin{aligned}
\mu_{\max}(t) &= \mu^0_{\max}\left[1 + p_{\mu_{\max}}\Theta_{\mu_{\max}}\left(\omega_{\mu_{\max}}t\right)\right],\\
K_{\mathrm{i}}(t) &= K^0_{\mathrm{i}}\left[1 + p_{K_{\mathrm{i}}}\Theta_{K_{\mathrm{i}}}\left(\omega_{K_{\mathrm{i}}}t\right)\right],\\
K_{\mathrm{s}}(t) &= K^0_{\mathrm{s}}\left[1 + p_{K_{\mathrm{s}}}\Theta_{K_{\mathrm{s}}}\left(\omega_{K_{\mathrm{s}}}t\right)\right],
\end{aligned} \tag{11}$$

where: $\mu^0_{\max}$, K^0_{i}, K^0_{s} are the mean values of growth rate function parameters; $p_{(\cdot)}$ denotes the grade of particular parameter uncertainty; $\Theta_{(\cdot)}$ stands for the periodic, continuous function; $\omega_{(\cdot)}$ signifies the frequency of particular parameter values changing. In this case $\Theta_{(\cdot)}$, $p_{(\cdot)}$ and $\omega_{(\cdot)}$ are assumed as follows:

$$\begin{aligned}
\Theta_{\mu_{\max}} &= \sin(\cdot),\ \omega_{\mu_{\max}} = 0.001,\ p_{\mu_{\max}} = 0.05,\\
\Theta_{K_{\mathrm{i}}} &= \cos(\cdot),\ \omega_{K_{\mathrm{i}}} = 0.014,\ p_{K_{\mathrm{i}}} = 0.05,\\
\Theta_{K_{\mathrm{s}}} &= \sin(\cdot),\ \omega_{K_{\mathrm{s}}} = 0.015,\ p_{K_{\mathrm{s}}} = 0.05.
\end{aligned} \tag{12}$$

In order to clarify the above description, the graphical representation of the cognitive model of considered processes in the CSTR is shown in Fig. 1.

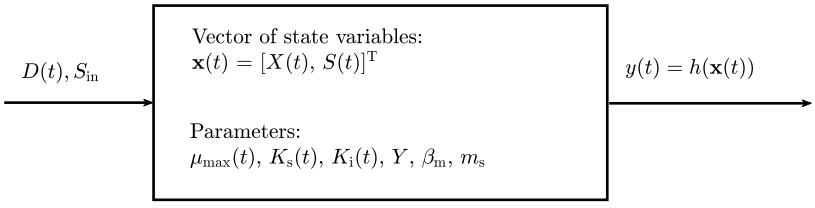

Figure 1: The graphical representation of the cognitive model of CSTR.

The devised observer provides the estimate of the unknown aggregated substrate concentration $S(t)$ from measurements of the aggregated biomass concentration $X(t)$ with using an appropriate model for estimation purposes.

4. Sliding mode observer - background

The certain crucial facts necessary for the clarity of presentation of the devised sliding mode observer are given in this section. In turn, the details of this general approach can be found in [13, 25, 36, 39, 40]. Thus, this section is aimed at presenting the theoretical background and highlighting against it all the relevant issues applicable for further considerations. The SMOs enable effective estimation of the state of uncertain dynamic systems. By connecting concepts of using the 'proportional' gain, e.g., from the Luenberger algorithm with the switching conditions from sliding mode algorithms, the proposed SMO provides two main features. Firstly, asymptotically tracking of the state trajectories $\boldsymbol{x}(t)$ is ensured. Secondly, the impact of the unknown term $\Delta(\boldsymbol{x}(t),t)$ on entire dynamics is compensated.

Hence, the considered SMO is able to not only asymptotic reconstructing of the original state but also 'estimating' uncertainty by equivalent control term [13, 36]. Clearly, by invoking to the classical observability rank theorem [4, 38, 42, 50, 51] and also matching condition [13, 36, 52], based on checking a relative degree of $\Delta(\boldsymbol{x}(t), t)$ with respect to the output $y(t)$, it is possible to use a sliding mode component to make uncertainty rejected. Therefore, it is possible to decouple the unknown part of dynamics from the estimation error by using sliding mode term to compensate the impact of the $\Delta(\boldsymbol{x}(t), t)$ (the unknown input is coupled with output due to matching condition whereas its undesired impact is decoupled from state estimates) [13]. According to [13, 25, 36, 39, 40], the general form of SMO for system Σ_{c} (Σ_{CSTR}) can be written as follows:

$$\begin{cases} \dot{\hat{\boldsymbol{x}}}(t) & = \hat{\boldsymbol{f}}(\hat{\boldsymbol{x}}(t)) + \boldsymbol{b}(\hat{\boldsymbol{x}}(t))u(t) + \left[\dfrac{\partial \boldsymbol{\Phi}}{\partial \hat{\boldsymbol{x}}}\right]^{-1} \left[\boldsymbol{K}^{\mathrm{SMO}}(y(t) - h(\hat{\boldsymbol{x}}(t)))\right] + \dfrac{1}{\tilde{\rho}_1(\hat{\boldsymbol{x}}(t))}\boldsymbol{\rho}(\hat{\boldsymbol{x}}(t))L^{\mathrm{SMO}}\mathrm{sgn}(y(t) - h(\hat{\boldsymbol{x}}(t))) \\ \hat{\boldsymbol{x}}(t) & = \hat{\boldsymbol{x}}_0 \end{cases}, \quad (13)$$

where: $\forall t \in \mathbb{T}: \ \hat{\boldsymbol{x}}(t) \in \mathbb{X}_{\mathrm{n}} \subset \mathbb{R}^{\mathrm{n}}$ denotes the vector of estimated state variables; $\boldsymbol{\Phi}$ is the non-linear state transformation; $\boldsymbol{K}^{\mathrm{SMO}} > \boldsymbol{0}^{\mathrm{n}\times 1}$, $L^{\mathrm{SMO}} > 0$ signify the gains vector of proportional part of SMO and the scalar gain of sliding part of SMO, respectively; $\tilde{\rho}_1(\cdot)$ is the first element of $\tilde{\boldsymbol{\rho}}(\cdot)$; $\mathrm{sgn}(\cdot)$ denotes signum function; $\dfrac{\partial(\cdot)}{\partial(\cdot)}$ is a partial derivative operator.

Considering (2), the non-linear state transformation $\boldsymbol{\Phi}: \mathbb{X}_{\mathrm{n}} \to \tilde{\mathbb{X}}_{\mathrm{n}}$ is defined as:

$$\tilde{\boldsymbol{x}}(t) = \boldsymbol{\Phi}(\boldsymbol{x}(t)) = \begin{bmatrix} h & L_{\hat{f}}h & \cdots & L_{\hat{f}}^{n-1}h \end{bmatrix}^{\mathrm{T}}, \quad (14)$$

where: $\tilde{\mathbb{X}}_{\mathrm{n}} \subset \mathbb{R}^{\mathrm{n}}$ signifies a 'new', n–dimensional connected manifold of analogous properties to $\mathbb{X}_{\mathrm{n}}$; $\forall t \in \mathbb{T}: \ \tilde{\boldsymbol{x}}(t) \in \tilde{\mathbb{X}}_{\mathrm{n}} \subset \mathbb{R}^{\mathrm{n}}$ is the vector of state variables in the 'new' coordinates; $L_{(\cdot)}^{(\cdot)}(\cdot)$ denotes Lie derivative [42, 53].

It is known that the state (coordinates) transformation is closely related to the observability of the considered system. Typically, for the synthesis of non-linear observers, the considered type of observability is understood by means of a distinguishing feature. There are many definitions associated with the essential understanding of distinguishable sets [38, 42, 50, 51, 54, 55]. For instance the uniform observability is related to the observability of all system states regardless of control input impact whereas strong observability is associated with observability of all states in a situation when unknown input appears in the system dynamics. In this work, due to the fact of action of sliding mode term, the observability is considered in classic, local, weak, and uniform manner.

Hence, in order to prove that (2) is observable it is needed to establish that observability co–distribution of one forms $d\mathcal{O} = \mathrm{span}\left\{ dh,\ dL_{\hat{f}}h,\ \ldots dL_{\hat{f}}^{n-1}h: \ h,\ L_{\hat{f}}h,\ \ldots L_{\hat{f}}^{n-1}h \in \mathcal{O} \right\}$, where $\mathcal{O} \subset C^{\infty}\left(\mathbb{X}_{\mathrm{n}}\right)$ is a linear observation space defined over field of $\mathbb{R}$ fulfil a dimension condition $\dim(d\mathcal{O}) = n$, $\forall t \in \mathbb{T}\ \boldsymbol{x}(t) \in \mathbb{X}_{\mathrm{n}}$, what means that reveal non-singularity and bijectivity properties [42, 53]. For the considered system, when output is decoupled from impact of inputs and the matching condition holds, the linear observation space is based on subsequent Lie derivatives of output equation $h(\cdot)$ with respect to vector field $\hat{\boldsymbol{f}}(\cdot)$. By imposing local coordinates into $\mathcal{O}$, the coordinates $(\boldsymbol{\Phi}(\boldsymbol{x}(t)))$ transformation is given by (14). Therefore, a co–distribution $d\mathcal{O}$ coincides with the Jacobian of non-linear state transformation. Henceforth, this Jacobian is called observability matrix and it is given as:

$$\dot{\tilde{\boldsymbol{x}}}(t) = \frac{\partial \boldsymbol{\Phi}}{\partial \boldsymbol{x}}(\boldsymbol{x}(t)) = \begin{bmatrix} dh \\ dL_{\hat{f}}h \\ \vdots \\ dL_{\hat{f}}^{n-1}h \end{bmatrix} = \begin{bmatrix} \nabla h \\ \nabla L_{\hat{f}}h \\ \vdots \\ \nabla L_{\hat{f}}^{n-1}h \end{bmatrix}, \quad (15)$$

where $d(\cdot)$ and $\nabla(\cdot)$ are an exterior derivative operator and a vector differential operator, respectively.

When the observability condition is fulfilled the observer structure (13) can be transformed into the following form:

$$\begin{cases} \dot{\hat{\tilde{\boldsymbol{x}}}}(t) & = \boldsymbol{A}\hat{\tilde{\boldsymbol{x}}}(t) + \tilde{\boldsymbol{\psi}}\left(\hat{\tilde{\boldsymbol{x}}}(t), u(t)\right) + \boldsymbol{K}^{\mathrm{SMO}}\left(y(t) - \boldsymbol{C}\hat{\tilde{\boldsymbol{x}}}(t)\right) + \tilde{\boldsymbol{\rho}}\left(\hat{\tilde{\boldsymbol{x}}}(t)\right)u_{\mathrm{r}}(t) \\ \hat{\tilde{\boldsymbol{x}}}(t_0) & = \hat{\tilde{\boldsymbol{x}}}_0 \end{cases}, \quad (16)$$

where: $\forall t \in \mathbb{T}:\ \hat{\tilde{\boldsymbol{x}}}(t) \in \tilde{\mathbb{X}}_{\mathrm{n}} \subset \mathbb{R}^{\mathrm{n}}$ denotes the vector of estimated state variables in the 'new' coordinates; $\boldsymbol{A} \in \mathbb{R}^{\mathrm{n}\times\mathrm{n}}$ and $\boldsymbol{C} \in \mathbb{R}^{1\times\mathrm{n}}$ are the constant matrices of the linear part of dynamics and outputs, respectively and they are considered as a parts of Brunovsky controllable canonical form [42, 50]; $\tilde{\boldsymbol{\psi}}:\ \tilde{\mathbb{X}}_{\mathrm{n}} \times \boldsymbol{U}_{\mathrm{p}} \to T\tilde{\mathbb{X}}_{\mathrm{n}}$, $\tilde{\boldsymbol{\rho}}:\ \tilde{\mathbb{X}}_{\mathrm{n}} \to T\tilde{\mathbb{X}}_{\mathrm{n}}$ denote the non-linear mapping defined as:

$$\tilde{\boldsymbol{\psi}}\left(\tilde{\boldsymbol{x}}(t), u(t)\right) = \tilde{\boldsymbol{\alpha}}(\tilde{\boldsymbol{x}}(t)) + \tilde{\boldsymbol{\gamma}}(\tilde{\boldsymbol{x}}(t))u(t), \tag{17}$$

and

$$\tilde{\boldsymbol{\rho}}(\tilde{\boldsymbol{x}}(t)) = [\tilde{\rho}_1(\tilde{x}_1(t))\ \ldots\ \tilde{\rho}_{i_{\mathrm{n}}}(\tilde{x}_1(t),\ \ldots\ ,\tilde{x}_{i_{\mathrm{n}}}(t))\ \ldots\ \tilde{\rho}_n(\tilde{\boldsymbol{x}}(t))]^{\mathrm{T}}\quad , \tag{18}$$

where:

$\tilde{\boldsymbol{\alpha}}(\tilde{\boldsymbol{x}}(t)) = \left[0\quad 0\quad \ldots\quad 0\quad \phi(\tilde{\boldsymbol{x}}(t)) = \left[L_{\hat{f}}^{n} h\right]\Big|_{\boldsymbol{x}=\boldsymbol{\Phi}^{-1}(\tilde{\boldsymbol{x}})}\right]^{\mathrm{T}}$,

$\tilde{\boldsymbol{\gamma}}(\tilde{\boldsymbol{x}}(t)) = [\tilde{\gamma}_1(\tilde{x}_1(t))\ \ldots\ \tilde{\gamma}_{i_{\mathrm{n}}}(\tilde{x}_1(t),\ \ldots\ ,\tilde{x}_{i_{\mathrm{n}}}(t))\ \ldots\ \tilde{\gamma}_n(\tilde{\boldsymbol{x}}(t))]^{\mathrm{T}}$,

$\tilde{\gamma}_{i_{\mathrm{n}}}(\cdot) = \left[L_{\boldsymbol{b}} L_{\hat{f}}^{i_{\mathrm{n}}-1} h\right]\Big|_{\boldsymbol{x}=\boldsymbol{\Phi}^{-1}(\tilde{\boldsymbol{x}})}$,

$\tilde{\rho}_{i_{\mathrm{n}}}(\cdot) = \left[L_{\rho} L_{\hat{f}}^{i_{\mathrm{n}}-1} h\right]\Big|_{\boldsymbol{x}=\boldsymbol{\Phi}^{-1}(\tilde{\boldsymbol{x}})}$, $i_{\mathrm{n}} = \overline{1,n}$;

$\boldsymbol{\Phi}^{-1}(\tilde{\boldsymbol{x}}(t))$ is the inverse Jacobi matrix of $\boldsymbol{\Phi}(\boldsymbol{x}(t))$ and $\tilde{\boldsymbol{\alpha}}$, $\tilde{\boldsymbol{\gamma}}$ and $\tilde{\boldsymbol{\rho}}$ are claimed as a bounded and locally Lipschitz on the set $\tilde{\mathbb{X}}_{\mathrm{n}}$.

In turn, the sliding mode term ($u_{\mathrm{r}}(t)$) from (13) in the new coordinates is determined as:

$$u_{\mathrm{r}}(t) = \frac{1}{\tilde{\rho}_1(\hat{\tilde{\boldsymbol{x}}}(t))} L^{\mathrm{SMO}} \mathrm{sgn}\left(y(t) - \boldsymbol{C}\hat{\tilde{\boldsymbol{x}}}(t)\right). \tag{19}$$

It is for two reasons. Firstly, it is connected with the fulfilling condition of a relative degree of measured output and secondly with introducing the sliding mode term into the observer dynamics [13, 25, 36, 39, 40].

By performing proper coordinates transformation, the observability of a given system can be claimed as independent of the input $u(t)$. In the literature it is called uniform observability [16, 42, 50, 51, 54]. According to the triangular form of (16) in the new coordinates, the following conditions must be hold [13]:

$$1 + \frac{\partial \tilde{\psi}_{i_{\mathrm{n}}}}{\partial \tilde{x}_{i_{\mathrm{n}}+1}} \neq 0,\ \frac{\partial \tilde{\rho}_{i_{\mathrm{n}}}}{\partial \tilde{x}_{i_{\mathrm{n}}+1}} \neq 0,\ i_{\mathrm{n}} = \overline{1, n-1}. \tag{20}$$

The conditions (20) assure that the dynamics of the considered system is uniformly observable. Moreover, the 'observability' of unknown input $\Delta(\boldsymbol{x}(t), t)$ must be examined. In the case, when $\Delta(\boldsymbol{x}(t), t)$ is involved in the differential equation established as derivative of the measured output $y(t)$, the sliding mode term, after reaching the sliding surface (equivalent control - $u_{\mathrm{r}}(t)$) can reconstruct the unknown part of the system dynamics [25, 28, 40]. To be more detailed, the equivalent control can 'estimate' the unknown input, only when the relative degree of measured output is equal to one, what means that the first order Lie derivative of the output equation $h(\cdot)$ is non zero: $\tilde{\rho}_1(\cdot) = L_{\rho} h \neq 0,\ \forall t \in \mathbb{T}$. It also means that in this variant of the SMO observer, the involutive of co–distribution associated with the $\tilde{\boldsymbol{\rho}}(\boldsymbol{x}(t))$ is not considered at all. For instance the idea of the sliding mode observer proposed in [28] is premised on the performing of non-linear transformation and also fulfilling the Frobenius theorem to make unknown inputs decoupled from the system dynamics in the new coordinates [25, 42].

It should be added that the above–presented methodology requires that the unknown inputs are structurally replaced by the sliding mode terms, which causes not affecting the disturbance to states of the system. If the proper transformation cannot be determined for the observability of the unknown inputs, the considered method can only proceed to obtain bounded estimation error. Moreover, the existence of the UIO SMO relies on the 'observability' of the unknown input. If the assumption of the relative degree of measured output does not hold, the unknown input cannot be reconstructed and the observer is not able to overcome the negative impact of the unknown dynamics [25, 36, 39, 40].

According to [13, 25, 36, 39, 40] tuning of the observer gains are strictly linked with establishing Lipschitz as well as bounding constants, which are used for the Lyapunov functions assessment. The main problem of the considered approach is that the values of the gain matrix $\boldsymbol{K}^{\mathrm{SMO}}$ strictly depend on the Lipschitz and bounding constants which

cannot be arbitrarily large. Therefore, fulfilling stability conditions is related to not only the selection of the values of $\boldsymbol{K}^{\mathrm{SMO}}$ in the left–half of the complex plane but also to values of above–mentioned constants [56–59]. More specifically, the clear relation between spectrum of the matrix $\boldsymbol{A}_{\boldsymbol{K}^{\mathrm{SMO}}} = \boldsymbol{A} - \boldsymbol{K}^{\mathrm{SMO}}\boldsymbol{C}$ and the maximal eigenvalue $\lambda_{\max}\left(\boldsymbol{\mathcal{P}}_{(\cdot)}\right)$, where $\boldsymbol{\mathcal{P}}_{(\cdot)}$ is a symmetric positive–definite matrix, in not particularly checked. However, due to the fact that the form of $\boldsymbol{A}$ and $\boldsymbol{C}$ coincides with the canonical form, there is a possibility of performing certain investigations. The important observations on this issue for an exemplary two–dimensional system are set out in appendix B.

In this paper, in comparison to the methodology presented in [13, 25, 36, 39, 40] authors proved that sliding mode term can not only reject the negative impact of the disturbances or the components of dynamics which parameters are time–variant (e.g. uncertain kinetics of biochemical processes), but also deals with unstructured uncertainty. It means that by proper choice of $\hat{\boldsymbol{f}}(\boldsymbol{x}(t))$ the unmodelled system dynamics is transferred into $\Delta(\boldsymbol{x}(t), t)$ and finally compensated by the sliding mode term.

5. Model of the considered system for SMO synthesis

Taking into account the information from section 4, it can be noticed that the cognitive model of considered biochemical processes presented in section 3 is not adequate for observer synthesis purposes. It is due to the excessive complexity of its structure. Clearly, this complexity might cause potential difficulties in analysing the stability of the designed SMO. Moreover, there are significant uncertainties in the structure of the cognitive model. Thus, it is not possible to derive the state (coordinates) transformation of the cognitive model with Haldane kinetics function due to the fact, there is no a bijectivity of the state transformation (relevant considerations on this issue are presented in appendix A). It is worth adding that this particular switch between two kinetics function allow to make state space fully observable due to fulfilling observability condition and also 'tracking' of uncertainity. In fact, due to inhibition effects which are imposed by Haldane kinetics, the sliding mode component must be applied to compensate unknown part of dynamics. Hence, a new (utility) model of a considered system for estimation purposes is needed. Therefore, the following assumptions are introduced in order to derive the utility model of the system Σ_{CSTR}:

- the structure of the specific growth rate function $\mu_{\mathrm{H}}(t)$ is replaced by the simplified Monod function $\hat{\mu}_{\mathrm{M}}(t)$ defined as:

$$\hat{\mu}_{\mathrm{M}}(t) = \mu^{0}_{\max}\frac{x_2(t)}{K^{0}_{\mathrm{s}} + x_2(t)}, \tag{21}$$

- whereas $\mu^{0}_{\max}$ and K^{0}_{s} are the estimates of uncertain parameters $\mu_{\max}(t)$ and $K_{\mathrm{s}}(t)$, respectively (see (11)).

To perform the observer synthesis, the state variables and inputs are defined as:

$$x_1(t) \triangleq X(t),\ x_2(t) \triangleq S(t),\ u(t) \triangleq D(t). \tag{22}$$

Finally, the utility model $\Sigma^{\mathrm{OS}}_{\mathrm{CSTR}}$ reads:

$$\Sigma^{\mathrm{OS}}_{\mathrm{CSTR}}:\begin{cases}\dot{x}_1(t) &= \hat{\mu}_{\mathrm{M}}(t)x_1(t) - \beta_{\mathrm{m}}x_1(t) - x_1(t)u(t) + \Delta(\boldsymbol{x}(t), t)\\ \dot{x}_2(t) &= -\dfrac{1}{Y}\hat{\mu}_{\mathrm{M}}(t)x_1(t) - m_{\mathrm{s}}x_1(t) + (S_{\mathrm{in}} - x_2(t))u(t) - \dfrac{1}{Y}\Delta(\boldsymbol{x}(t), t)\\ \boldsymbol{x}(t_0) &= x_0\\ y(t) &= x_1(t)\end{cases}. \tag{23}$$

It should be noted that the proposed function (21) substituting kinetics function enables a proper state transformation as well as a relatively good mapping of the real behaviour of the original system (cognitive model). The comparison between the cognitive and utility model is presented in section 7.1. Moreover, the analysis of potential usage of Haldane function in the utility model is shown in appendix A.

The components $\hat{\boldsymbol{f}}(\boldsymbol{x}(t))$ and $\boldsymbol{b}(\boldsymbol{x}(t))$ of model (23) are equal to:

$$\begin{aligned}\hat{\boldsymbol{f}}(\boldsymbol{x}(t)) &= \begin{bmatrix}\hat{\mu}_{\mathrm{M}}(t)x_1(t) - \beta_{\mathrm{m}}x_1(t)\\ -\dfrac{1}{Y}\hat{\mu}_{\mathrm{M}}(t)x_1(t) - m_{\mathrm{s}}x_1(t)\end{bmatrix},\\ \boldsymbol{b}(\boldsymbol{x}(t)) &= \begin{bmatrix}-x_1(t)\\ S_{\mathrm{in}} - x_2(t)\end{bmatrix}.\end{aligned} \tag{24}$$

It is worth adding that typically only component representing kinetics function in a non-linear model of considered biochemical processes is treated as highly uncertain. Therefore, the uncertain part of the system $\Sigma^{\mathrm{OS}}_{\mathrm{CSTR}}$, which holds the necessary conditions for SMO synthesis is determined as:

$$\begin{aligned}\Delta(\boldsymbol{x}(t),t) &= \left[\mu_{\mathrm{H}}(t) - \hat{\mu}_{\mathrm{M}}(t)\right] x_1(t),\\ \boldsymbol{\rho}(\boldsymbol{x}(t)) &= \begin{bmatrix} 1 \\ -\dfrac{1}{Y} \end{bmatrix}.\end{aligned} \tag{25}$$

Remark 1. Considering the general facts about the problem of uncertainty in function $\mu_{(\cdot)}(t)$, authors claims, that the proposed approach of using simplified Monod function (21) to ensure holding the observability condition might be extended to the wider class of models, which describe the dynamics of bioreactors.

Remark 2. As it has been mentioned above, the significance of growth rates impact on the dynamics of biochemical processes is unbeatable. Some papers, e.g., [11, 31, 34, 35] presents methodological and application considerations on handling the general issue of both state and unknown input estimation in the context of the biochemical system. This work provides some new ideas for this field. By assuming that kinetics function appears in all of the dynamical equations of the considered system, using the sliding mode term in observer dynamics causes compensation not only the negative impact of 'bad' input but also its estimation. Taking into account that in sliding phase the uncertain part of system dynamics is 'estimated' by the sgn(·) function $\Delta(\boldsymbol{x}(t),t) \approx \mathrm{sgn}(-\varepsilon_1(t))_{\mathrm{eq}}$, it may be concluded that due to the nature of $\Delta(\boldsymbol{x}(t),t)$ established for considered class of biochemical system, the sliding mode observer is able to reconstruct the behaviour of function $\mu(t)$. More specifically, when the sliding mode term reaches the sliding surface, its operation causes the current value of $u_{\mathrm{r}}(t)$ given by (19) to map the value of $\Delta(\boldsymbol{x}(t),t)$. Thus, knowing that by applying transformation (3), and in particular (25) the conditions of applicability of the SMO are satisfied, the following transformation is possible. Hence, given the structure of the $\Delta(\boldsymbol{x}(t),t)$ in (25), $\forall t \in \mathbb{T}$ the values of $x_1(t)$, $x_2(t)$, $\mu^0_{\max}$, and K^0_{s} are known or can be reconstructed on-line. Thus, in order to determine the analytical formula for calculating $\mu_{\mathrm{H}}(t)$, one must compare $\Delta(\boldsymbol{x}(t),t)$ with the sliding mode term. For instance in the considered example (6), by taking form of kinetics function $\hat{\mu}_{\mathrm{M}}(t)$ from (21), and $\Delta(\boldsymbol{x}(t),t)$ from (25) the following assessment $\tilde{\mu}_{\mathrm{H}}(t)$ of $\mu_{\mathrm{H}}(t)$ is obtained:

$$\forall t \in \mathbb{T}\ \hat{x}_1(t) \neq 0 \rightarrow \tilde{\mu}_{\mathrm{H}}(t) \quad \approx \frac{1}{\hat{x}_1(t)} \mathrm{sgn}(y(t) - h(\hat{\boldsymbol{x}}(t)))_{\mathrm{eq}} + \hat{\mu}_{\mathrm{M}}(t), \tag{26}$$

where $\mathrm{sgn}(y(t) - h(\hat{\boldsymbol{x}}(t)))_{\mathrm{eq}}$ is the equivalent control of the sliding mode term [52].

Thus, uncertainty compensation occurs by satisfying the matching condition – coupling the uncertainty modelled as an unknown input to a differentiable (in the sense of Lie derivatives – relative order of output equal to one) measurement output. This results in the unknown input being 'observable' due to the operation of the sliding mode term. On the other hand, in the SMO structure, the uncertain input is replaced by the sliding mode term. Thus, one obtains the ability to accurately track the uncertainty, and through appropriate transformations, e.g. (26), to determine the kinetics function of the original system.

6. Design of sliding mode observer for the CSTR

The state (coordinates) transformation for system (23) is as follows:

$$\tilde{\boldsymbol{x}}(t) = \boldsymbol{\Phi}(\boldsymbol{x}(t)) = \begin{bmatrix} x_1(t) \\ \hat{\mu}_{\mathrm{M}}(t)x_1(t) - \beta_{\mathrm{m}}x_1(t) \end{bmatrix} = \begin{bmatrix} x_1(t) \\ \dfrac{t_1(t)}{t_2(t)}x_1(t) - \beta_{\mathrm{m}}x_1(t) \end{bmatrix}, \tag{27}$$

which in $\mathbb{X}_{\mathrm{n}}$ coordinates space is always non–singular due to persistent non–negativeness of $x_2(t)$, where $t_1(t) = \mu^0_{\max}x_2(t)$ and $t_2(t) = K^0_{\mathrm{s}} + x_2(t)$.

Making simple calculations the inverse coordinates transformation yields:

$$\boldsymbol{x}(t) = \boldsymbol{\Phi}^{-1}(\tilde{\boldsymbol{x}}(t)) = \begin{bmatrix} \tilde{x}_1(t) \\ \dfrac{-K^0_{\mathrm{s}}\left(\tilde{x}_2(t) + \beta_{\mathrm{m}}\tilde{x}_1(t)\right)}{\tilde{x}_2(t) + \beta_{\mathrm{m}}\tilde{x}_1(t) - \mu^0_{\max}\tilde{x}_1(t)} \end{bmatrix}, \tag{28}$$

which is non–singular in the whole space $\tilde{\mathbb{X}}_{\mathrm{n}}$ excluding set $\{\forall t \in \mathbb{T}\ \tilde{\boldsymbol{x}}(t) \in \tilde{\mathbb{X}}_{\mathrm{n}} :\ \tilde{x}_2(t) + \beta_{\mathrm{m}}\tilde{x}_1(t) - \mu^0_{\max}\tilde{x}_1(t) = 0\}$.

Taking into account (27) the Jacobi matrix of transformation between $\mathbb{X}_{\mathrm{n}}$ and $\tilde{\mathbb{X}}_{\mathrm{n}}$ is calculated as follows:

$$d\tilde{\boldsymbol{x}}(t) = \frac{\partial \boldsymbol{\Phi}}{\partial \boldsymbol{x}}(\boldsymbol{x}(t)) = \begin{bmatrix} 1 & 0 \\ \dfrac{t_1(t)}{t_2(t)} - \beta_{\mathrm{m}} & \dfrac{t_3(t)K^0_{\mathrm{s}}}{\left(t_2(t)\right)^2} \end{bmatrix}, \tag{29}$$

where $t_3(t) = \mu^0_{\max}x_1(t)$,

and its determinant is given as:

$$\det\left[\frac{\partial \boldsymbol{\Phi}}{\partial \boldsymbol{x}}\right] = \frac{t_3(t)K^0_{\mathrm{s}}}{\left(t_2(t)\right)^2}. \tag{30}$$

Remark 3. It should be noted that the obtained determinant (30) indicates that the transformation between state spaces is singular in the set $\mathcal{S}_{\mathrm{Ob}} = \left\{\boldsymbol{x}(t) \in \Omega :\ x_1(t) = 0\right\} \subset \Omega$. It means that the considered system is not observable in the whole space Ω. Due to the fact that the point $\left\{\mathbf{0}_{2\times 1}\right\} \subset \mathcal{S}_{\mathrm{Ob}}$ is strictly linked with the certain important dynamical features of the model (23) [37], it is necessary to establish a region where the proper operations of the designed SMO is ensured. Because of the singularity of (29) only in the one particular case, it is needed to prove that the system dynamics cannot reach the set $\mathcal{S}_{\mathrm{Ob}}$. Due to its continuous action in time this is indeed. It is tantamount to stating that the considered system is observable in the set $\Omega \setminus \left\{\mathbf{0}_{2\times 1}\right\}$.

Using (29) and (30) the inverse Jacobi matrix can be rewritten as:

$$\left[\frac{\partial \boldsymbol{\Phi}}{\partial \boldsymbol{x}}\right]^{-1} = \begin{bmatrix} 1 & 0 \\ t_2(t)\dfrac{t_4 + t_5(t) - t_1(t)}{t_3(t)K^0_{\mathrm{s}}} & \dfrac{\left(t_2(t)\right)^2}{t_3(t)K^0_{\mathrm{s}}} \end{bmatrix}, \tag{31}$$

where $t_4 = K^0_{\mathrm{s}}\beta_m$ and $t_5(t) = \beta_{\mathrm{m}}x_2(t)$.

In turn, using (17) the mapping $\tilde{\boldsymbol{\alpha}}(\boldsymbol{x}(t))$ reads:

$$\tilde{\boldsymbol{\alpha}}(\boldsymbol{x}(t)) = \begin{bmatrix} 0 \\ \dfrac{\left(t_4 + t_5(t) - t_1(t)\right)^2}{\left(t_2(t)\right)^2}x_1(t) - \tilde{\boldsymbol{\alpha}}(\boldsymbol{x}(t))_{(2)} \end{bmatrix}, \tag{32}$$

where $t_6 = Ym_{\mathrm{s}}$;

$$\tilde{\boldsymbol{\alpha}}(\boldsymbol{x}(t))_{(2)} = \frac{t_3(t)K^0_{\mathrm{s}}x_1(t)\left(t_1(t) + K^0_{\mathrm{s}}t_6 + t_6x_2(t)\right)}{Y\left(t_2(t)\right)^3},$$

whereas the mapping $\tilde{\boldsymbol{\gamma}}(\boldsymbol{x}(t))$ yields:

$$\tilde{\boldsymbol{\gamma}}(\boldsymbol{x}(t)) = \begin{bmatrix} -x_1(t) \\ x_1(t)\left(\beta_{\mathrm{m}} - \dfrac{t_1(t)}{t_2(t)}\right) + \tilde{\boldsymbol{\gamma}}(\boldsymbol{x}(t))_{(2)} \end{bmatrix}, \tag{33}$$

where $\tilde{\boldsymbol{\gamma}}(\boldsymbol{x}(t))_{(2)} = \left(\dfrac{t_3(t)}{t_2(t)} - \dfrac{t_1(t)x_1(t)}{\left(t_2(t)\right)^2}\right)\left(S_{\mathrm{in}} - x_2(t)\right)$,

and the mapping $\tilde{\boldsymbol{\rho}}(\boldsymbol{x}(t))$ linked with uncertainty is as follows:

$$\tilde{\boldsymbol{\rho}}(\boldsymbol{x}(t)) = \begin{bmatrix} 1 \\ \dfrac{t_1(t)}{t_2(t)} - \left(\dfrac{t_3(t)}{Yt_2(t)} - \dfrac{t_1(t)x_1(t)}{Y\left(t_2(t)\right)^2}\right) - \beta_{\mathrm{m}} \end{bmatrix}. \tag{34}$$

Hence, the dynamics of the designed SMO in the new coordinates $\tilde{\boldsymbol{x}}(t)$, by invoking to (16) is derived as:

$$\begin{cases} \dot{\hat{\tilde{x}}}_1(t) & = \tilde{\alpha}_1(\tilde{\boldsymbol{x}}(t)) + \tilde{\gamma}_1(\tilde{\boldsymbol{x}}(t))u(t) + K_1^{\mathrm{SMO}}(y(t) - \hat{\tilde{x}}_1(t)) + \tilde{\rho}_1(\tilde{\boldsymbol{x}}(t))L^{\mathrm{SMO}}\mathrm{sgn}(y(t) - \hat{\tilde{x}}_1(t)) \\ \dot{\hat{\tilde{x}}}_2(t) & = \tilde{x}_1(t) + \tilde{\alpha}_2(\tilde{\boldsymbol{x}}(t)) + \tilde{\gamma}_2(\tilde{\boldsymbol{x}}(t))u(t) + K_1^{\mathrm{SMO}}(y(t) - h(\hat{\boldsymbol{x}}(t))) + K_2^{\mathrm{SMO}}(y(t) - \hat{\tilde{x}}_1(t)) \\ & \quad + \tilde{\rho}_2(\tilde{\boldsymbol{x}}(t))L^{\mathrm{SMO}}\mathrm{sgn}(y(t) - \hat{\tilde{x}}_1(t)) \\ \hat{\tilde{\boldsymbol{x}}}(t_0) & = \hat{\tilde{\boldsymbol{x}}}_0 \\ y(t) & = \tilde{x}_1(t) \end{cases}, \tag{35}$$

where the state, outputs and gains matrices are equal to:

$$\boldsymbol{A} = \begin{bmatrix} 0 & 1 \\ 0 & 0 \end{bmatrix}, \ \boldsymbol{C} = \begin{bmatrix} 1 & 0 \end{bmatrix}, \ \boldsymbol{K}^{\mathrm{SMO}} = \begin{bmatrix} K_1^{\mathrm{SMO}} \\ K_2^{\mathrm{SMO}} \end{bmatrix}, \tag{36}$$

and the mappings from (32), (33) and (34) are expressed in the new coordinates as: $\tilde{\boldsymbol{\alpha}}(\tilde{\boldsymbol{x}}(t)) = \left[\tilde{\boldsymbol{\alpha}}(\boldsymbol{x}(t))\right]\Big|_{\boldsymbol{x}=\boldsymbol{\Phi}^{-1}(\tilde{\boldsymbol{x}})}$, $\tilde{\boldsymbol{\gamma}}(\tilde{\boldsymbol{x}}(t)) = \left[\tilde{\boldsymbol{\gamma}}(\boldsymbol{x}(t))\right]\Big|_{\boldsymbol{x}=\boldsymbol{\Phi}^{-1}(\tilde{\boldsymbol{x}})}$, $\tilde{\boldsymbol{\rho}}(\tilde{\boldsymbol{x}}(t)) = \left[\tilde{\boldsymbol{\rho}}(\boldsymbol{x}(t))\right]\Big|_{\boldsymbol{x}=\boldsymbol{\Phi}^{-1}(\tilde{\boldsymbol{x}})}$.

The SMO structure (35) is used for stability analysis purposes. In turn, the SMO structure in the original coordinates (37) is used for implementation purposes. This structure is delivered by invoking to (13) incorporating the inverse Jacobi matrix (31) and it is as follows:

$$\begin{cases} \dot{\hat{x}}_1(t) & = \hat{\mu}_{\mathrm{M}}(t)\hat{x}_1(t) - \beta_{\mathrm{m}}\hat{x}_1(t) - \hat{x}_1(t)u(t) + K_1^{\mathrm{SMO}}(y(t) - h(\boldsymbol{x}(t))) + L^{\mathrm{SMO}}\mathrm{sgn}(y(t) - h(\boldsymbol{x}(t))) \\ \dot{\hat{x}}_2(t) & = -\frac{1}{Y}\hat{\mu}_{\mathrm{M}}(t)\hat{x}_1(t) - m_{\mathrm{s}}\hat{x}_1(t) + (S_{\mathrm{in}} - \hat{x}_2(t))u(t) + O_1(t)K_2^{\mathrm{SMO}}(y(t) - h(\boldsymbol{x}(t))) + O_2(t)K_1^{\mathrm{SMO}}(y(t) - h(\boldsymbol{x}(t))) \\ & \quad -\frac{1}{Y}L^{\mathrm{SMO}}\mathrm{sgn}(y(t) - h(\boldsymbol{x}(t))) \\ \hat{\boldsymbol{x}}(t_0) & = \hat{\boldsymbol{x}}_0 \\ y(t) & = h(\boldsymbol{x}(t)) = x_1(t) \end{cases}, \tag{37}$$

where $O_1(t) = \dfrac{(K_{\mathrm{s}}^0 + \hat{x}_2(t))^2}{\mu_{\max}^0 K_{\mathrm{s}}^0 \hat{x}_1(t)}$ and $O_2(t) = \left(K_{\mathrm{s}}^0 + \hat{x}_2(t)\right)\dfrac{K_{\mathrm{s}}^0\beta_{\mathrm{m}} + \beta_{\mathrm{m}}\hat{x}_2(t) - \mu_{\max}^0\hat{x}_2(t)}{\mu_{\max}^0 K_{\mathrm{s}}^0 \hat{x}_1(t)}$.

Theorem 1. The sliding mode observer (37) produces stable and robust estimates $\hat{x}_1(t)$ and $\hat{x}_2(t)$ of the state variables $x_1(t)$ and $x_2(t)$, respectively in spite of the parametric and unstructured uncertainty in the system dynamics.

Proof. The estimation error ($\boldsymbol{\varepsilon}(t) \triangleq \hat{\boldsymbol{x}}(t) - \boldsymbol{x}(t)$) in the new coordinates $\forall t \in \mathbb{T}: \ \tilde{\boldsymbol{\varepsilon}}(t) \in \tilde{\boldsymbol{E}}_{\mathrm{n}} \subset \mathbb{R}^{\mathrm{n}}$ can be written as:

$$\tilde{\boldsymbol{\varepsilon}}(t) \triangleq \hat{\tilde{\boldsymbol{x}}}(t) - \tilde{\boldsymbol{x}}(t) = \boldsymbol{\Phi}(\hat{\boldsymbol{x}}(t)) - \boldsymbol{\Phi}(\boldsymbol{x}(t)). \tag{38}$$

First, the boundedness of the estimation error, i.e. $\forall t \in \mathbb{T}: \ ||\tilde{\boldsymbol{\varepsilon}}(t)|| \leq \tilde{\boldsymbol{\varepsilon}}^{\max} \in \mathbb{R}_+$ during reaching the sliding surface is demonstrated. It should be noted that in this situation the first element of this estimation error vector, i.e. $\tilde{\varepsilon}_1(t)$ pursues zero. Thus, as in [36], the following Lyapunov function $\boldsymbol{V}_1(\cdot)$ can be defined:

$$\boldsymbol{V}_1(\tilde{\boldsymbol{\varepsilon}}(t)) = \tilde{\boldsymbol{\varepsilon}}^{\mathrm{T}}(t)\boldsymbol{\mathcal{P}}_1\tilde{\boldsymbol{\varepsilon}}(t), \tag{39}$$

where $\boldsymbol{\mathcal{P}}_1 = \boldsymbol{\mathcal{P}}_1^{\mathrm{T}} \in \mathbb{R}^{\mathrm{n}\times\mathrm{n}}$ is a symmetric positive–definite matrix.

Using (35) and (23) expressed in the new coordinates, the estimation error dynamics can be written as:

$$\dot{\tilde{\boldsymbol{\varepsilon}}}(t) = \underbrace{\boldsymbol{A}_{\boldsymbol{K}^{\mathrm{SMO}}}\tilde{\boldsymbol{\varepsilon}}(t)}_{\text{the linear part of estimation error}} + \underbrace{\tilde{\boldsymbol{\psi}}_{\mathrm{d}} + \tilde{\boldsymbol{\rho}}_{\mathrm{d}}}_{\substack{\text{the bounded and Lipschitz} \\ \text{non-linear functions}}}, \tag{40}$$

where: $\tilde{\boldsymbol{\psi}}_{\mathrm{d}} = \tilde{\boldsymbol{\psi}}(\hat{\tilde{\boldsymbol{x}}}(t), u(t)) - \tilde{\boldsymbol{\psi}}(\tilde{\boldsymbol{x}}(t), u(t))$; $\tilde{\boldsymbol{\rho}}_{\mathrm{d}} = \tilde{\boldsymbol{\rho}}(\hat{\tilde{\boldsymbol{x}}}(t))u_{\mathrm{r}}(t) - \tilde{\boldsymbol{\rho}}(\tilde{\boldsymbol{x}}(t))\Delta(\boldsymbol{x}(t), t)$; $\tilde{\boldsymbol{\psi}}(\tilde{\boldsymbol{x}}(t), u(t))$, $u_{\mathrm{r}}(t)$, and $\Delta(\boldsymbol{x}(t), t)$ are taken from (17), (19) and (25), respectively.

Owing to (40) the derivative of the Lyapunov function (39) reads:

$$\dot{V}_1(\tilde{\boldsymbol{\varepsilon}}(t)) = \dot{\tilde{\boldsymbol{\varepsilon}}}^{\mathrm{T}}(t)\boldsymbol{\mathcal{P}}_1\tilde{\boldsymbol{\varepsilon}}(t) + \tilde{\boldsymbol{\varepsilon}}^{\mathrm{T}}(t)\boldsymbol{\mathcal{P}}_1\dot{\tilde{\boldsymbol{\varepsilon}}}(t) = \tilde{\boldsymbol{\varepsilon}}^{\mathrm{T}}(t)\left[\left(\boldsymbol{A}_{\boldsymbol{K}^{\mathrm{SMO}}}\right)^{\mathrm{T}}\boldsymbol{\mathcal{P}}_1 + \boldsymbol{\mathcal{P}}_1\boldsymbol{A}_{\boldsymbol{K}^{\mathrm{SMO}}}\right]\tilde{\boldsymbol{\varepsilon}}(t) + 2\tilde{\boldsymbol{\varepsilon}}^{\mathrm{T}}(t)\boldsymbol{\mathcal{P}}_1\tilde{\boldsymbol{\psi}}_{\mathrm{d}} + 2\tilde{\boldsymbol{\varepsilon}}^{\mathrm{T}}(t)\boldsymbol{\mathcal{P}}_1\tilde{\boldsymbol{\rho}}_{\mathrm{d}}. \quad (41)$$

If (41) is strictly negative, the global boundedness of the estimation error (38) is guaranteed [25]. It should be noted that, in general, the component of a given $\dot{V}_{(\cdot)}(\tilde{\boldsymbol{\varepsilon}}(t))$ associated with the linear part of estimation error (see (40)) can be assessed using the Lyapunov equation [43]:

$$\tilde{\boldsymbol{\varepsilon}}^{\mathrm{T}}(t)\left[\left(\boldsymbol{A}_{\boldsymbol{K}^{\mathrm{SMO}}}\right)^{\mathrm{T}}\boldsymbol{\mathcal{P}}_{(\cdot)} + \boldsymbol{\mathcal{P}}_{(\cdot)}\boldsymbol{A}_{\boldsymbol{K}^{\mathrm{SMO}}}\right]\tilde{\boldsymbol{\varepsilon}}(t) = -\tilde{\boldsymbol{\varepsilon}}^{\mathrm{T}}(t)\boldsymbol{\mathcal{Q}}_{(\cdot)}\tilde{\boldsymbol{\varepsilon}}(t), \quad (42)$$

where $\boldsymbol{\mathcal{Q}}_{(\cdot)} \in \mathbb{R}^{\mathrm{n}\times\mathrm{n}}$ is a symmetric positive–definite matrix and $\boldsymbol{\mathcal{P}}_{(\cdot)}$ shall be interpreted as in (39).

Typically, it is assumed that the matrix $\boldsymbol{\mathcal{Q}}_{(\cdot)}$ is the identity matrix of proper dimension, therefore the proper choice of the observer gains matrix ensures negative–definite matrix of the linear part of estimation error dynamics [4, 13, 36, 56, 57]. Hence, taking into account the above, the remaining components of the derivative of the Lyapunov function may be assessed as follows [4, 13, 19, 25, 36, 39, 40, 56, 57, 60]:

$$\left\|\tilde{\boldsymbol{\psi}}_{\mathrm{d}}\right\| \leq L_{\tilde{\boldsymbol{\psi}}}\left\|\tilde{\boldsymbol{\varepsilon}}(t)\right\|, \ \left\|\tilde{\boldsymbol{\rho}}_{\mathrm{d}}\right\| \ \leq \beta_{\tilde{\rho}}\left(\overline{\Delta} + L^{\mathrm{SMO}}\beta_{\mathrm{u_r}}\right), \quad (43)$$

where: $L_{\tilde{\boldsymbol{\psi}}} \geq 0$ is the (real) Lipschitz constant of functional $\tilde{\boldsymbol{\psi}}(\tilde{\boldsymbol{x}}(t), u(t))$; $\beta_{\tilde{\rho}} \geq 0$ denotes the (real) bounding constant of the function $\tilde{\boldsymbol{\rho}}(\hat{\tilde{\boldsymbol{x}}}(t))$; $\beta_{\mathrm{u_r}} \geq 0$ stands for the (real) bounding constant of the function $\dfrac{1}{\tilde{\rho}(\tilde{\boldsymbol{x}}(t))}$.

The methodology for determining the bounding and Lipschitz constants is presented in appendix C.

Combining (41), (42) and (43), $\dot{V}_1(\tilde{\boldsymbol{\varepsilon}}(t))$ can assessed by [13, 36, 56, 57, 61]:

$$\dot{V}_1(\tilde{\boldsymbol{\varepsilon}}(t)) \leq -\left\|\tilde{\boldsymbol{\varepsilon}}(t)\right\|^2 + 2\lambda_{\max}\left(\boldsymbol{\mathcal{P}}_1\right)L_{\tilde{\boldsymbol{\psi}}}\left\|\tilde{\boldsymbol{\varepsilon}}(t)\right\|^2 + 2\lambda_{\max}\left(\boldsymbol{\mathcal{P}}_1\right)\left(\overline{\Delta} + L^{\mathrm{SMO}}\beta_{\mathrm{u_r}}\right)\left\|\tilde{\boldsymbol{\varepsilon}}(t)\right\| < 0, \quad (44)$$

where $\lambda_{\max}\left(\boldsymbol{\mathcal{P}}_{(\cdot)}\right)$ is the maximal eigenvalue of the Lyapunov matrix (see also appendix B).

Transformation (44) provides to:

$$0 < \left\|\tilde{\boldsymbol{\varepsilon}}(t)\right\| < \frac{2\lambda_{\max}\left(\boldsymbol{\mathcal{P}}_1\right)\beta_{\tilde{\rho}}\left(\overline{\Delta} + L^{\mathrm{SMO}}\beta_{\mathrm{u_r}}\right)}{1 - 2\lambda_{\max}\left(\boldsymbol{\mathcal{P}}_1\right)L_{\tilde{\boldsymbol{\psi}}}}. \quad (45)$$

Finally, if $\forall t \in \mathbb{T}$:

$$\lambda_{\max}\left(\boldsymbol{\mathcal{P}}_1\right) < \frac{1}{2L_{\tilde{\boldsymbol{\psi}}}}, \quad (46)$$

the estimation error (38) is uniformly bounded [43].

Remark 4. It should be added that because of the different results of the numerical calculation of the Lipschitz constant $L_{\tilde{\boldsymbol{\psi}}}$ [56, 57] the following operation is necessary. Taking into account (17), $L_{\tilde{\boldsymbol{\psi}}}$ can be expressed as $L_{\tilde{\boldsymbol{\psi}}} = L_{\tilde{\boldsymbol{\alpha}}} + L_{\tilde{\boldsymbol{\gamma}}}u_{\mathrm{bound}}$, where $L_{\tilde{\boldsymbol{\alpha}}}$ and $L_{\tilde{\boldsymbol{\gamma}}}$ are Lipschitz constants of the non-linear components of the affine form (calculating according to appendix C). This transformation is possible due to applying the triangle inequality on (17) [43, 62].

During reaching the sliding surface ($\tilde{\varepsilon}_1(t)$ pursues zero) other elements of the estimation error vector $\tilde{\boldsymbol{\varepsilon}}(t)$ must be free from the uncertainty (impact of the switching operations). Thus, the adequate assignation of the sliding mode gain L^{SMO} is necessary. Because the sliding surface is $\tilde{\varepsilon}_1(t) = 0$, the proper design (19) gives the certainty of reaching and maintaining on the sliding surface [36]. By ensuring that $u_{\mathrm{r}}(t) - \Delta(\boldsymbol{x}(t), t)$ in (41) is in the sliding mode, the uncertainty can be replaced by the incremental component [13, 25, 36, 39].

In order to reach the sliding surface ($\tilde{\varepsilon}_1(t) = 0$) in the finite time the two following conditions must be fulfilled [36]:

$$L^{\mathrm{SMO}} > \frac{\tilde{\varepsilon}_2^{\max} + \overline{\Delta}}{\beta_{\mathrm{u_r}}}, \ K_1^{\mathrm{SMO}} \ > L_{\tilde{\gamma}_1}u_{\mathrm{bound}}, \quad (47)$$

where $\tilde{\varepsilon}_2^{\max} > 0$ is the maximal value of the second element $\tilde{\varepsilon}_2(t)$ of the vector of estimation error $\tilde{\boldsymbol{\varepsilon}}(t)$ and $L_{\tilde{\gamma}_1} > 0$ denotes the Lipschitz constant of the $\tilde{\gamma}_1(\cdot)$ from (17).

Combining (36) and (17), the $\tilde{\varepsilon}_1(t)$ dynamics can be written as [13, 36]:

$$\dot{\tilde{\varepsilon}}_1(t) = \tilde{\varepsilon}_2(t) + \tilde{\gamma}_{1\mathrm{d}} u(t) - K_1^{\mathrm{SMO}} \tilde{\varepsilon}_1(t) + u_{\mathrm{r}}(t) - \Delta(\boldsymbol{x}(t), t), \tag{48}$$

where $\tilde{\gamma}_{1\mathrm{d}} = \tilde{\gamma}_1(\hat{\tilde{x}}_1(t)) - \tilde{\gamma}_1(\tilde{x}_1(t))$.

Defining the Lyapunov function associated with $\tilde{\varepsilon}_1(t)$ as [13, 36]:

$$V_{\tilde{\varepsilon}_1}(\tilde{\varepsilon}_1(t)) = \frac{1}{2}\tilde{\varepsilon}_1^2(t), \tag{49}$$

its derivative reads:

$$\dot{V}_{\tilde{\varepsilon}_1}(\tilde{\varepsilon}_1(t)) = -K_1^{\mathrm{SMO}} \tilde{\varepsilon}_1^2(t) + \tilde{\varepsilon}_1(t)\tilde{\gamma}_{1\mathrm{d}} u(t) + \tilde{\varepsilon}_1(t)\left[\tilde{\varepsilon}_2(t) - \Delta(\boldsymbol{x}(t), t) + u_{\mathrm{r}}(t)\right]. \tag{50}$$

To explain the derivation of conditions (47) using (50), the two following inequalities are considered [13, 36]:

$$\begin{aligned} &-K_1^{\mathrm{SMO}} \tilde{\varepsilon}_1^2(t) + \tilde{\varepsilon}_1(t)\tilde{\gamma}_{1\mathrm{d}} u(t) < 0, \\ &\tilde{\varepsilon}_1(t)\left[\tilde{\varepsilon}_2(t) - \Delta(\boldsymbol{x}(t), t) - u_{\mathrm{r}}(t)\right] < 0. \end{aligned} \tag{51}$$

It is obvious that if $\forall t \in \mathbb{T}$ both inequalities (51) holds, then (50) is always negative. The holding of the first inequality of (51) is elementary and based on the following Lipschitz assessment:

$$-K_1^{\mathrm{SMO}} \tilde{\varepsilon}_1^2(t) + \tilde{\varepsilon}_1(t)\tilde{\gamma}_{1\mathrm{d}} u(t) \leq -K_1^{\mathrm{SMO}} \tilde{\varepsilon}_1^2(t) + L_{\tilde{\gamma}_1} u_{\mathrm{bound}} \tilde{\varepsilon}_1^2(t) < 0. \tag{52}$$

If the system dynamics is in the phase of reaching ($\tilde{\varepsilon}_1(t) \neq 0$), by eliminating the $\tilde{\varepsilon}_1^2(t)$ expression from (52), the inequality is transformed to K_1^{SMO} and the second condition from (47) is obtained. The explanation of the first condition from (47) is more complicated. The second inequality of (51) can be assessed as follows:

$$\tilde{\varepsilon}_1(t)\left[\tilde{\varepsilon}_2(t) - \Delta(\boldsymbol{x}(t), t) - u_{\mathrm{r}}(t)\right] \leq |\tilde{\varepsilon}_1(t)|\left[\tilde{\varepsilon}_2(t) - \Delta(\boldsymbol{x}(t), t) - u_{\mathrm{r}}(t)\right] < 0. \tag{53}$$

Taking into account that $|\tilde{\varepsilon}_1(t)|$ is always positive and bounded the rest of the inequality (53) must be investigated from point of view of always being negative. If the second condition from (47) is fulfilled, it remains to prove that the proper choice of the L^{SMO} involves convergence of $\tilde{\varepsilon}_1(t)$ to zero. Using suitable assessment on the particular elements, the following holds:

$$\beta_{\mathrm{u_r}} L^{\mathrm{SMO}} > |\tilde{\varepsilon}_2(t) - \Delta(\boldsymbol{x}(t), t)|. \tag{54}$$

Knowing that $\tilde{\varepsilon}_2(t)$ and $\Delta(\boldsymbol{x}(t), t)$ are time–varying and they are real numbers, in general, the right–hand side of inequality (54) must be assessed in the most conservative way. By establishing $\tilde{\varepsilon}_2^{\max}$ and $\overline{\Delta}$, the supremum of the right–hand side of (54) equals to the sum of bounding constants, which legitimates the first condition of (47). Hence, in the case when the both above–mentioned conditions holds, and if $\tilde{\varepsilon}_1(t) \neq 0$, the Lyapunov function $\forall t \in \mathbb{T}\ \dot{V}_{\tilde{\varepsilon}_1}(\tilde{\varepsilon}_1(t)) < 0$. Thus, to conclude the proper selection of the SMO gains ensures reaching, and thereafter maintaining on the sliding surface $\tilde{\varepsilon}_1(t) = 0$ [13, 36]. Moreover, when $\tilde{\varepsilon}_1(t)$ is in the sliding mode, then the additive sliding mode component can be considered as an 'estimator' (tracking element) for $\Delta(\boldsymbol{x}(t), t)$. Therefore, the switching term in the sliding mode is claimed as a compensating element for an unknown input and significantly improve the accuracy of obtained estimates.

As it has been above–mentioned, the proper choice of the SMO gains ensures the global boundedness of the estimation error. As soon as the trajectories of the estimation error reach the sliding surface, the dynamics of the estimation error $\tilde{\boldsymbol{\varepsilon}}(t)$ asymptotically converge to a zero equilibrium point [13, 36]. If the convergence of the error trajectories is ensured, the phenomena of equivalent control begin to interact with the observer dynamics [13, 17, 20, 36, 52]. Therefore, considering (48) in the sliding mode ($\tilde{\varepsilon}_1(t) = 0$) $u_{\mathrm{r}}(t)$ can be expressed as [13, 25, 36, 39, 40]:

$$u_{\mathrm{r}}(t) \equiv u_{\mathrm{eq}}(t) = \Delta(\boldsymbol{x}(t), t) - \tilde{\varepsilon}_2(t). \tag{55}$$

Hence, substituting (55) to (40) the dynamics of the estimation error can be rewritten as follows:

$$\dot{\tilde{\boldsymbol{\varepsilon}}}(t) = \underbrace{\boldsymbol{A}_{\boldsymbol{K}^{\mathrm{SMO}}}\tilde{\boldsymbol{\varepsilon}}(t)}_{\text{the linear part of estimation error}} + \underbrace{\tilde{\boldsymbol{\psi}}_{\mathrm{d}} + \left[\tilde{\boldsymbol{\rho}}(\hat{\tilde{\boldsymbol{x}}}(t)) - \tilde{\boldsymbol{\rho}}(\tilde{\boldsymbol{x}}(t))\right] u_{\mathrm{eq}}(t) - \tilde{\boldsymbol{\rho}}(\tilde{\boldsymbol{x}}(t))\tilde{\varepsilon}_2(t)}_{\text{the Lipschitz non–linear functions}}. \tag{56}$$

It is obvious that the equilibrium point of (56) is $\overline{\tilde{\boldsymbol{\varepsilon}}} = \mathbf{0}$, so its asymptotic stability must be ensured. To prove that the estimation error dynamics is stable in the sliding mode the following Lyapunov function $\boldsymbol{V}_2(\cdot)$ is defined [36]:

$$\boldsymbol{V}_2\left(\tilde{\boldsymbol{\varepsilon}}(t)\right) = \tilde{\boldsymbol{\varepsilon}}^{\mathrm{T}}(t)\boldsymbol{\mathcal{P}}_2\tilde{\boldsymbol{\varepsilon}}(t), \tag{57}$$

where $\boldsymbol{\mathcal{P}}_2 = \boldsymbol{\mathcal{P}}_2^{\mathrm{T}} \in \mathbb{R}^{\mathrm{n}\times\mathrm{n}}$ is a symmetric positive–definite matrix.

Owing to (56), the derivative of the Lyapunov function (57) reads:

$$\begin{aligned}\dot{V}_2(\tilde{\boldsymbol{\varepsilon}}(t)) = \dot{\tilde{\boldsymbol{\varepsilon}}}^{\mathrm{T}}(t)\boldsymbol{\mathcal{P}}_2\tilde{\boldsymbol{\varepsilon}}(t) + \tilde{\boldsymbol{\varepsilon}}^{\mathrm{T}}(t)\boldsymbol{\mathcal{P}}_2\dot{\tilde{\boldsymbol{\varepsilon}}}(t) = \tilde{\boldsymbol{\varepsilon}}^{T}(t)\left[\left(\boldsymbol{A}_{\boldsymbol{K}^{\mathrm{SMO}}}\right)^{\mathrm{T}}\boldsymbol{\mathcal{P}}_2 + \boldsymbol{\mathcal{P}}_2\boldsymbol{A}_{\boldsymbol{K}^{\mathrm{SMO}}}\right]\tilde{\boldsymbol{\varepsilon}}(t)\\ + 2\tilde{\boldsymbol{\varepsilon}}^{\mathrm{T}}(t)\boldsymbol{\mathcal{P}}_2\tilde{\boldsymbol{\psi}}_{\mathrm{d}} + 2\tilde{\boldsymbol{\varepsilon}}^{\mathrm{T}}(t)\boldsymbol{\mathcal{P}}_2\left(-\tilde{\boldsymbol{\rho}}(\tilde{\boldsymbol{x}}(t))\right)\tilde{\varepsilon}_2(t) + 2\tilde{\boldsymbol{\varepsilon}}^{\mathrm{T}}(t)\boldsymbol{\mathcal{P}}_2\left[\tilde{\boldsymbol{\rho}}(\hat{\tilde{\boldsymbol{x}}}(t)) - \tilde{\boldsymbol{\rho}}(\tilde{\boldsymbol{x}}(t))\right]u_{\mathrm{eq}}(t).\end{aligned} \tag{58}$$

Following the same procedure as for (43), the particular components of (58) can be assessed by the proper bounding and Lipschitz constants as follows [36]:

$$\begin{aligned}\left\|\tilde{\boldsymbol{\rho}}(\hat{\tilde{\boldsymbol{x}}}(t))u_{\mathrm{eq}}(t) - \tilde{\boldsymbol{\rho}}(\tilde{\boldsymbol{x}}(t))u_{\mathrm{eq}}(t)\right\| &\leq L_{\tilde{\rho}}\overline{u}_{\mathrm{eq}}\left\|\tilde{\boldsymbol{\varepsilon}}(t)\right\|,\\ \left\|\tilde{\boldsymbol{\rho}}(\tilde{\boldsymbol{x}}(t))\right\| &\leq \beta_{\tilde{\rho}},\end{aligned} \tag{59}$$

where $L_{\tilde{\rho}} > 0$ is the (real) Lipschitz constant of functional $\tilde{\boldsymbol{\rho}}(\tilde{\boldsymbol{x}}(t))$, $\overline{u}_{\mathrm{eq}} = \beta_{\mathrm{u_r}}L^{\mathrm{SMO}}$ is the (real) bounding constant of equivalent control term, whereas $\beta_{\tilde{\rho}} > 0$ is the (real) bounding constant of term $\tilde{\boldsymbol{\rho}}(\tilde{\boldsymbol{x}}(t))$.

Remark 5. In general, it should be noted that the problem of the appropriate selection of SMO gains is complexity. Clearly, according to the stability analysis of non-linear observers, the procedure of observer gains determining may be very distinct and non–trivial [13, 19, 43, 56, 57, 60, 63–65]. The presented considerations clearly show that the methodology of the selection of Lyapunov function has undoubtedly crucial meaning. Hence, taking into account the stability conditions, e.g, (46) and (47) it is possible that the observer works well (the generated estimates converge asymptotically and remarkably fast to their originals) even though the given global stability conditions are not retained [61].

Thus, analysing the designed SMO dynamics it is relatively easy to evaluate the stability of its linear part if the gains of $\boldsymbol{K}^{\mathrm{SMO}}$ matrix are known. However, it is not enough from the stability point of view, in general. Clearly, the conditions associated with the assessment of the non-linear part of error dynamics must be also fulfilled. As it is widely discussed in the literature, e.g., [13, 36, 56, 57, 61, 63, 65] the modification of the $\boldsymbol{K}^{\mathrm{SMO}}$ must guarantee that the Lyapunov matrix $\boldsymbol{\mathcal{P}}_{(\cdot)}$ is always positive–definite or even its maximal eigenvalue $\lambda_{\max}\left(\boldsymbol{\mathcal{P}}_{(\cdot)}\right)$ must be smaller than the given combination of the bounding or Lipschitz constants (see, e.g., (46)). In general, for the wide class of the linear dynamics such as, e.g., (36) it is very hard to claim what the values of $\boldsymbol{K}^{\mathrm{SMO}}$ influence on the eigenvalues of Lyapunov matrix. However, for the considered case, due to take into account the controllability canonical form and because the system is two–dimensional, it is possible to check this relationship, which is presented in appendix B. Of course this problem can be turn to the case, when the $\boldsymbol{K}^{\mathrm{SMO}}$ (which involves change of $\lambda_{\max}\left(\boldsymbol{\mathcal{P}}_{(\cdot)}\right)$ value) is given and determination of operating region is under investigation. This is strictly linked with evaluation of $\mathbb{X}_{\mathrm{n}}$ and $\tilde{\mathbb{X}}_{\mathrm{n}}$. If the values of bounding or Lipschitz constants cannot be optionally modified, the fulfilling of stability conditions are not possible [13, 56, 57]. Due to the methodology of determining of Lipschitz and bounding constants presented in appendix C, it should be highlighted that the way they are valued is undoubtedly important. This is because of the numerical or analytical approach to the calculation and it is also associated with preconceiving of the operating region of the considered system. Therefore, the obtained values of constants can be too 'conservative', and they may significantly influence the evaluation of stability conditions. Thus, a new approach to deriving stability conditions is proposed. Taking into account (42), (43) and (59) the derivative of the Lyapunov function (58) is dominated by the following, based on Schwarz and triangle inequalities [62], function:

$$\begin{aligned}\dot{V}_2(\tilde{\boldsymbol{\varepsilon}}(t)) \leq \tilde{\boldsymbol{\varepsilon}}^{\mathrm{T}}(t)\left[\left(\boldsymbol{A}_{\boldsymbol{K}^{\mathrm{SMO}}}\right)^{\mathrm{T}}\boldsymbol{\mathcal{P}}_2 + \boldsymbol{\mathcal{P}}_2\boldsymbol{A}_{\boldsymbol{K}^{\mathrm{SMO}}}\right]\tilde{\boldsymbol{\varepsilon}}(t) + 2L_{\tilde{\alpha}}\left\|\boldsymbol{\mathcal{P}}_2\tilde{\boldsymbol{\varepsilon}}(t)\right\|\left\|\tilde{\boldsymbol{\varepsilon}}(t)\right\| + 2\beta_{\tilde{\rho}}\left\|\boldsymbol{\mathcal{P}}_2\tilde{\boldsymbol{\varepsilon}}(t)\right\|\left|\tilde{\varepsilon}_2(t)\right|\\ + 2L_{\tilde{\gamma}}u_{\mathrm{bound}}\left\|\boldsymbol{\mathcal{P}}_2\tilde{\boldsymbol{\varepsilon}}(t)\right\|\left\|\tilde{\boldsymbol{\varepsilon}}(t)\right\| + 2L_{\tilde{\rho}}\overline{u}_{\mathrm{eq}}\left\|\boldsymbol{\mathcal{P}}_2\tilde{\boldsymbol{\varepsilon}}(t)\right\|\left\|\tilde{\boldsymbol{\varepsilon}}(t)\right\|,\end{aligned} \tag{60}$$

where particular components, taking into account $|\tilde{\varepsilon}_2(t)| \leq ||\tilde{\boldsymbol{\varepsilon}}(t)||$, can be assessed by:

$$2L_{\tilde{\alpha}}\left|\left|\boldsymbol{\mathcal{P}}_2\tilde{\boldsymbol{\varepsilon}}(t)\right|\right|\left|\left|\tilde{\boldsymbol{\varepsilon}}(t)\right|\right| \leq L_{\tilde{\alpha}}^2\tilde{\boldsymbol{\varepsilon}}^{\mathrm{T}}(t)\boldsymbol{\mathcal{P}}_2\boldsymbol{\mathcal{P}}_2\tilde{\boldsymbol{\varepsilon}}(t) + \tilde{\boldsymbol{\varepsilon}}^{\mathrm{T}}(t)\tilde{\boldsymbol{\varepsilon}}(t),$$

$$2\beta_{\tilde{\rho}}\left|\left|\boldsymbol{\mathcal{P}}_2\tilde{\boldsymbol{\varepsilon}}(t)\right|\right|\left|\tilde{\varepsilon}_2(t)\right| \leq \beta_{\tilde{\rho}}^2\tilde{\boldsymbol{\varepsilon}}^{\mathrm{T}}(t)\boldsymbol{\mathcal{P}}_2\boldsymbol{\mathcal{P}}_2\tilde{\boldsymbol{\varepsilon}}(t) + \tilde{\varepsilon}_2^2(t) \leq \beta_{\tilde{\rho}}^2\tilde{\boldsymbol{\varepsilon}}^{\mathrm{T}}(t)\boldsymbol{\mathcal{P}}_2\boldsymbol{\mathcal{P}}_2\tilde{\boldsymbol{\varepsilon}}(t) + \tilde{\boldsymbol{\varepsilon}}^{\mathrm{T}}(t)\tilde{\boldsymbol{\varepsilon}}(t),$$

$$2L_{\tilde{\gamma}}u_{\mathrm{bound}}\left|\left|\boldsymbol{\mathcal{P}}_2\tilde{\boldsymbol{\varepsilon}}(t)\right|\right|\left|\left|\tilde{\boldsymbol{\varepsilon}}(t)\right|\right| \leq L_{\tilde{\gamma}}^2u_{\mathrm{bound}}^2\tilde{\boldsymbol{\varepsilon}}^{\mathrm{T}}(t)\boldsymbol{\mathcal{P}}_2\boldsymbol{\mathcal{P}}_2\tilde{\boldsymbol{\varepsilon}}(t) + \tilde{\boldsymbol{\varepsilon}}^{\mathrm{T}}(t)\tilde{\boldsymbol{\varepsilon}}(t),$$

$$2L_{\tilde{\rho}}\overline{u}_{\mathrm{eq}}\left|\left|\boldsymbol{\mathcal{P}}_2\tilde{\boldsymbol{\varepsilon}}(t)\right|\right|\left|\left|\tilde{\boldsymbol{\varepsilon}}(t)\right|\right| \leq L_{\tilde{\rho}}^2\overline{u}_{\mathrm{eq}}^2\tilde{\boldsymbol{\varepsilon}}^{\mathrm{T}}(t)\boldsymbol{\mathcal{P}}_2\boldsymbol{\mathcal{P}}_2\tilde{\boldsymbol{\varepsilon}}(t) + \tilde{\boldsymbol{\varepsilon}}^{\mathrm{T}}(t)\tilde{\boldsymbol{\varepsilon}}(t). \tag{61}$$

Using (61), (60) can be written as follows:

$$\begin{aligned}\dot{V}_2(\tilde{\boldsymbol{\varepsilon}}(t)) \leq{}& \tilde{\boldsymbol{\varepsilon}}^{\mathrm{T}}(t)\left[\left(\boldsymbol{A}_{\boldsymbol{K}^{\mathrm{SMO}}}\right)^{\mathrm{T}}\boldsymbol{\mathcal{P}}_2 + \boldsymbol{\mathcal{P}}_2\boldsymbol{A}_{\boldsymbol{K}^{\mathrm{SMO}}}\right]\tilde{\boldsymbol{\varepsilon}}(t) + L_{\tilde{\alpha}}^2\tilde{\boldsymbol{\varepsilon}}^{\mathrm{T}}(t)\boldsymbol{\mathcal{P}}_2\boldsymbol{\mathcal{P}}_2\tilde{\boldsymbol{\varepsilon}}(t) + \beta_{\tilde{\rho}}^2\tilde{\boldsymbol{\varepsilon}}^{\mathrm{T}}(t)\boldsymbol{\mathcal{P}}_2\boldsymbol{\mathcal{P}}_2\tilde{\boldsymbol{\varepsilon}}(t)\\ &+ L_{\tilde{\gamma}}^2u_{\mathrm{bound}}^2\tilde{\boldsymbol{\varepsilon}}^{\mathrm{T}}(t)\boldsymbol{\mathcal{P}}_2\boldsymbol{\mathcal{P}}_2\tilde{\boldsymbol{\varepsilon}}(t) + L_{\tilde{\rho}}^2\overline{u}_{\mathrm{eq}}^2\tilde{\boldsymbol{\varepsilon}}^{\mathrm{T}}(t)\boldsymbol{\mathcal{P}}_2\boldsymbol{\mathcal{P}}_2\tilde{\boldsymbol{\varepsilon}}(t) + 4\tilde{\boldsymbol{\varepsilon}}^{\mathrm{T}}(t)\tilde{\boldsymbol{\varepsilon}}(t).\end{aligned} \tag{62}$$

By eliminating the vector of estimation error from (62) the following matrix inequality is obtained:

$$\left(\boldsymbol{A}_{\boldsymbol{K}^{\mathrm{SMO}}}\right)^{\mathrm{T}}\boldsymbol{\mathcal{P}}_2 + \boldsymbol{\mathcal{P}}_2\boldsymbol{A}_{\boldsymbol{K}^{\mathrm{SMO}}} + \left[L_{\tilde{\alpha}}^2 + \beta_{\tilde{\rho}}^2 + L_{\tilde{\gamma}}^2u_{\mathrm{bound}}^2 + L_{\tilde{\rho}}^2\overline{u}_{\mathrm{eq}}^2\right]\boldsymbol{\mathcal{P}}_2\boldsymbol{\mathcal{P}}_2 + 4\boldsymbol{I} < 0, \tag{63}$$

which solution with respect to the matrix $\boldsymbol{\mathcal{P}}_2$ guarantees the global asymptotic stability of the designed SMO.

Hence, the sliding mode observer (37) is the stable and robust estimator guaranteeing that $\hat{x}_1(t)$ and $\hat{x}_2(t)$ are the estimates of the state variables $x_1(t)$ and $x_2(t)$, respectively despite the parametric and unstructured uncertainty in the system dynamics. □

Remark 6. The theorem 1 has been proven in a similar way to [13, 25, 36, 39, 40]. However, the wider uncertainty has been taken into account which leads to certain interesting conclusions and remarks. Moreover, all significant differences from [13, 25, 36, 39, 40] have been precisely indicated.

Remark 7. It is well–known that for sliding techniques the chattering problem appears [52]. In the literature there are several approaches to the reduction of this phenomenon. In this work, a method premised on an approximation of signum function by the following, continuous function is used [13, 20, 36]:

$$\mathrm{sgn}(\varepsilon_1(t)) \approx \varphi_{\mathrm{sgn}}(\varepsilon_1(t), \varepsilon_{\mathrm{sgn}}) = \frac{\varepsilon_1(t)}{\left|\varepsilon_1(t)\right| + \varepsilon_{\mathrm{sgn}}}, \tag{64}$$

where $\varepsilon_{\mathrm{sgn}} > 0$ is a real tuning parameter.
Hence, when the sliding mode appears the uncertainty $\Delta(\boldsymbol{x}(t), t)$ is approximated by $\varphi_{\mathrm{sgn}}(\varepsilon_1(t), \varepsilon_{\mathrm{sgn}})$ and the accuracy of this operation strictly depends on the value of $\varepsilon_{\mathrm{sgn}}$. If this value is too small, the behaviour of the function may reveal rapid changes of values (but not as much as in the case of 'real' chattering), whereas when this value is too big the approximation of sliding mode action is impaired [52]. The trajectories of approximating function $\varphi_{\mathrm{sgn}}(\varepsilon_1(t), \varepsilon_{\mathrm{sgn}})$ depend on the selection of the three example values of the parameter $\varepsilon_{\mathrm{sgn}}$ are presented in Fig. 2. It is worth adding that, in the context of the sliding mode term as well as its approximating function, it is important to emphasise that the selection of the value of gain L^{SMO} must be related not only with the fulfilment of the stability conditions (45), (54), and (63) but also must be selected in such a way to prevent occurrence of the so-called peaking phenomenon [12, 16, 19, 43, 66, 67]. This phenomenon might lead to the fact that the estimates generated by the SMO have large values at the beginning of the estimation process. Also might appear long transient states, high sensitivity to measurement noises or external disturbances, or even loss of stability of the observer. Due to the numerical aspects and the fact that the value of L^{SMO} is constant, the software implementation of the signum function and its approximation may lead to the peaking phenomenon. Thus, the proper selection of the gain L^{SMO} and $\varepsilon_{\mathrm{sgn}}$ is necessary because it enables satisfying stability conditions, reducing chattering, ensuring high quality of state reconstruction, and preventing peaking phenomenon.

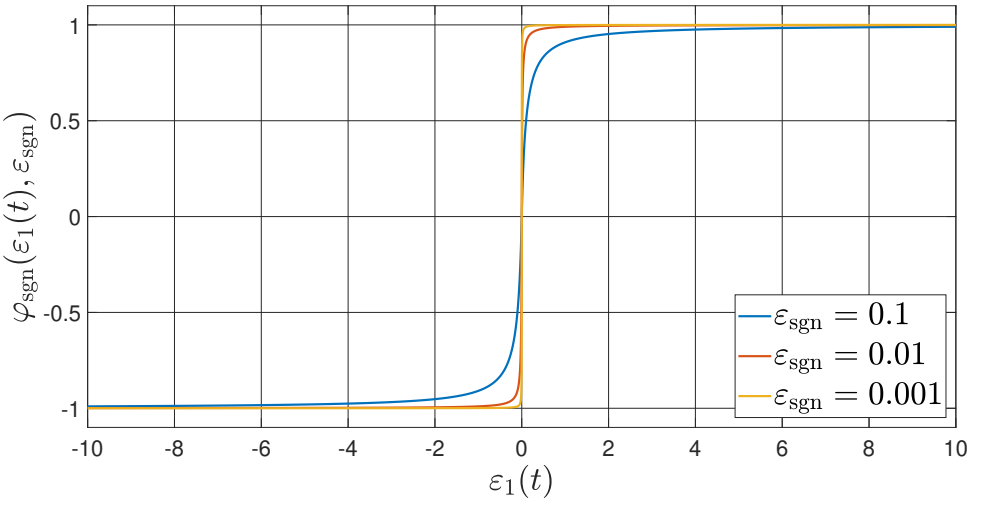

Figure 2: The trajectories of approximating function $\varphi_{\mathrm{sgn}}(\varepsilon_1(t), \varepsilon_{\mathrm{sgn}})$.

Table 1
The values of the model parameters

No.	Parameter	Value	Unit
1.	β_{m}	0.02	h^{-1}
2.	$\mu_{\max}(t)$	[0.315 ; 0.3465]	h^{-1}
3.	$\mu_0(t)$	[0.6277 ; 0.6723]	h^{-1}
5.	$D(t)$	[0.01 ; 0.05]	h^{-1}
6.	$K_{\mathrm{i}}(t)$	[23.75 ; 26.25]	g/L
7.	$K_{\mathrm{s}}(t)$	[4.75 ; 5.25]	g/L
8.	m_{s}	0.01	h^{-1}
9.	S_{in}	5	g/L
10.	Y	0.5	–

7. Case study

The sliding mode observer (37) has been applied to the model of CSTR (6). The entire system has been implemented and validated in Matlab/Simulink environmental. The values of the particular parameters, assuming a 5% uncertainty calculated from their mean value, are shown in table 1 [45]. Their variability is determined by (11) and (12). Hence, it can be noticed that certain parameters are burden by parametric uncertainty. Moreover, according to section 5 there is also unstructured uncertainty. Therefore, the comparison between the cognitive (6) and utility (23) models is presented and discussed at the beginning of this section. In turn, the estimation results are investigated in the second part of case study.

7.1. Comparison between bioreactor models

In this work, it is assumed that the cognitive model (6) is a satisfactory representation of reality. In turn, the need to devise the utility model is discussed in detail and analysed in section 5. In this section, a simulation analysis of the dynamics behaviour of both models is presented. In order to make a proper comparison, the same control signal has been applied to both models. Its trajectory is presented in Fig. 3. It is worth adding that due to permanent inflow of wastewater to bioreactor represents by $u(t)$ in both cases the dynamics of the considered system has not reached the equilibrium point $\{\mathbf{0}_{2\times 1}\}$, which it means that $\forall t \in \mathbb{T}$ the region of proper action of the observer is kept.

In turn, the trajectories of $\mu_{(\cdot)}(t)$ for the cognitive and utility model are shown in Fig. 4. As it can be noticed, the

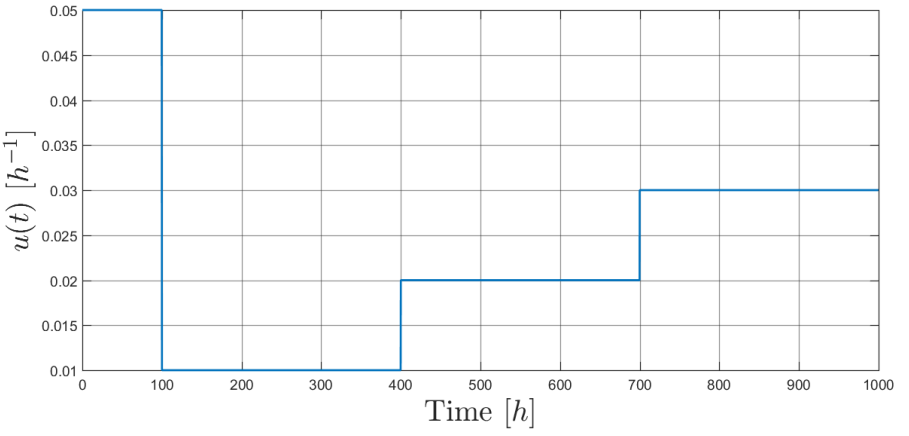

Figure 3: Trajectory of the control signal applied to both models.

trajectories are similar, but even a small difference between them has a significant impact on the trajectories of state variables. These trajectories, from the initial conditions $\boldsymbol{x}(0) = \begin{bmatrix}1 & 0.5\end{bmatrix}^{\mathrm{T}}$, are presented in Figs. 5 and 6 for $x_1(t)$ and $x_2(t)$, respectively.

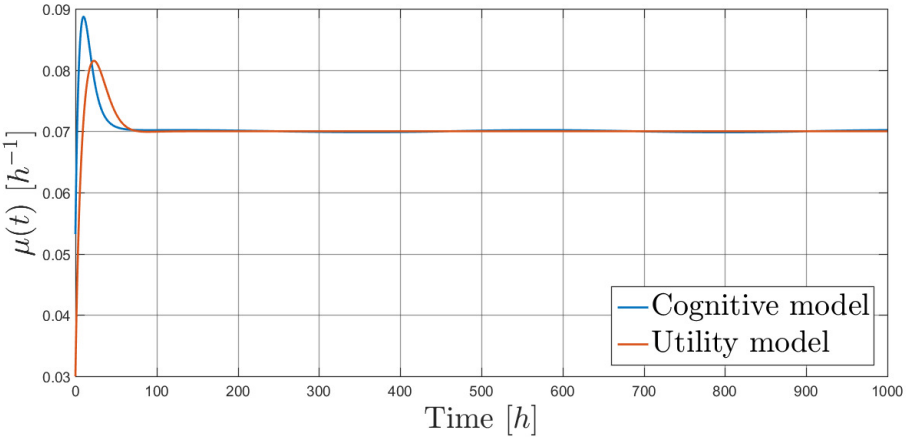

Figure 4: Trajectories of $\mu_{(\cdot)}(t)$ obtained from the cognitive and utility model of CSTR.

As it easy to observe in Figs. 5 and 6 the slight difference in kinetics involves significantly different evaluation of the state vector over time in both models. Thus, it can be noticed what extensive uncertainty the designed SMO has to deal with in order to reconstruct satisfactorily the state of the considered system. However, as it has been mentioned in section 5 to fulfil the observability condition this level of mismatch between the cognitive and utility model have to be claimed as acceptable.

7.2. Implementation of the sliding mode observer

In this section, all essential numerical aspects related to the designed SMO are first presented. In turn, the trajectories of the generated estimates of the state variables and discussion of the accuracy of the estimation are included in its last part.

7.2.1. Numerical aspects

Taking into account conditions delivered in section 6 the SMO gains, i.e. $\boldsymbol{K}^{\mathrm{SMO}}$ and $\boldsymbol{L}^{\mathrm{SMO}}$ should be distinctly selected. Dealing with this task is inevitably associated with the calculation of the bounding and Lipschitz constants, which are needed to assess certain particular vector or scalar variables. The realisation of this task needs to perform

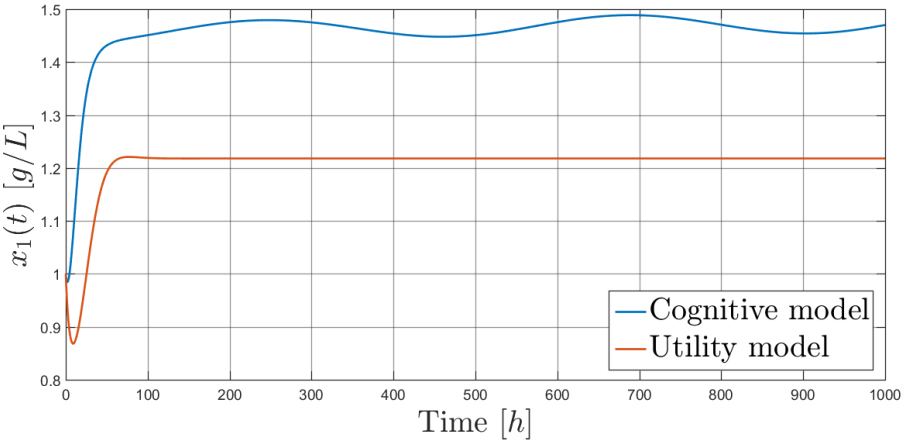

Figure 5: Trajectories of the state variable $x_1(t)$ obtained from cognitive and utility model of CSTR.

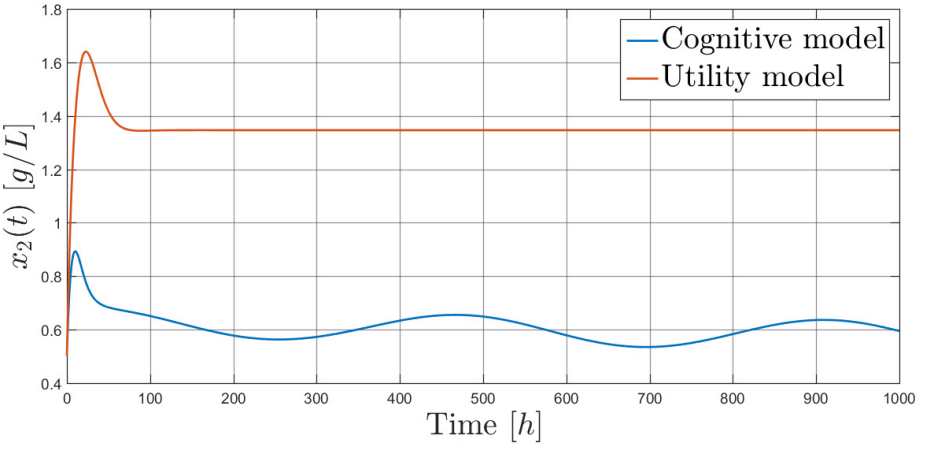

Figure 6: Trajectories of the state variable $x_2(t)$ obtained from cognitive and utility model of CSTR.

assessment the time–varying: vectors of state, estimation error, and control input as well as values of parameters. Methodology of the bounding and Lipschitz constants calculation presented in appendix C is based on numerical approach, hence apart of knowing the analytical formulae of the particular relationships, e.g., $\tilde{\boldsymbol{\alpha}}(\cdot)$, $\Delta(\boldsymbol{x}(t), t)$ the bounds on particular signals have to be employed.

The constant bounding the control input and extreme values of the parameters of kinetics function (11) are easy to establish, however, the calculation of all Lipschitz and bounding constants is much more difficult. According to appendix C the convex hyper–cubes of the state variables and estimation error must be established for both 'original' and 'new' vector spaces. Let sets $\mathbb{X}_{\mathrm{n}}^{\mathrm{BL}} \subset \Omega \subset \mathbb{X}_{\mathrm{n}}$, $\tilde{\mathbb{X}}_{\mathrm{n}}^{\mathrm{BL}} \subset \tilde{\mathbb{X}}_{\mathrm{n}}$, $\boldsymbol{E}_{\mathrm{n}}^{\mathrm{BL}} \subset \boldsymbol{E}_{\mathrm{n}}$ and also $\tilde{\boldsymbol{E}}_{\mathrm{n}}^{\mathrm{BL}} \subset \tilde{\boldsymbol{E}}_{\mathrm{n}}$ stand for sets associated with operating region of the system dynamics. In general, the decomposition into subsets associated with a particular coordinate is linked with establishing the lower and upper bounds of the state and estimation error variables. This work has been done by numerical (simulation) analysis of the behaviour of both cognitive and utility models, which effects are presented in section 7.1. In fact, the sets $\mathbb{X}_{\mathrm{n}}^{\mathrm{BL}}$ and $\tilde{\mathbb{X}}_{\mathrm{n}}^{\mathrm{BL}}$ include not only the original state variables bounds but also extreme values of their estimates. Hence, the calculation of the bounding and Lipschitz constants is premised on utilising relatively conservative assessment of the system dynamics in the operating region. As it has been mentioned before, the assessment of the upper and lower bounds of the state and error variables have been done by simulation analysis of the system dynamics, however, for providing some 'safety' the extreme values have been selected as 'vaguely' wider. The establishing of bounds for the state and vector variables after the coordinates transformation has been performed by not only utilising derived transformation (27) but also assuming that the continuous function

which takes values in convex set is also convex [12, 62].

For the system (23) the hyper–cube established in the state space $\mathbb{X}_{\mathrm{n}}^{\mathrm{BL}}$ is given by:

$$0.8 \leq x_1(t) \leq 1.5,\ 0.5 \leq x_2(t) \leq 1. \tag{65}$$

In turn, using (27) the hyper–cube in the new state space (coordinates) $\tilde{\mathbb{X}}_{\mathrm{n}}^{\mathrm{BL}}$ is as follows:

$$0.8 \leq \tilde{x}_1(t) \leq 1.5,\ 0.008 \leq \tilde{x}_2(t) \leq 0.0525. \tag{66}$$

Similarly, for the system (23) the hyper–cube established in the error space $\boldsymbol{E}_{\mathrm{n}}^{\mathrm{BL}}$ is given by:

$$0.05 \leq \varepsilon_1(t) \leq 0.2,\ 0.05 \leq \varepsilon_2(t) \leq 0.6, \tag{67}$$

and the hyper–cube in the new error space $\tilde{\boldsymbol{E}}_{\mathrm{n}}^{\mathrm{BL}}$ is as follows:

$$0.05 \leq \tilde{\varepsilon}_1(t) \leq 0.2,\ \ -0.0033 \leq \tilde{\varepsilon}_2(t) \leq 0.0031. \tag{68}$$

Hence, using (65), (66), (67) and (68), the procedures for calculating the bounding and Lipschitz constants given in appendix C, and the values of parameters from table 1, the following constants are determined:

$$\begin{aligned} u_{\mathrm{bound}} = 0.05,\ L_{\tilde{\boldsymbol{\alpha}}} = 0.134,\ L_{\tilde{\boldsymbol{\gamma}}} = 3.9652, L_{\tilde{\boldsymbol{\psi}}} = 0.3323,\ L_{\tilde{\gamma}_1} = 1,\ L_{\tilde{\boldsymbol{\rho}}} = 2.1061,\ \beta_{\tilde{\boldsymbol{\rho}}} = 1.0133, \\ \beta_{\mathrm{u_r}} = 1,\ \overline{\Delta} = 0.0921,\ \tilde{\varepsilon}_2^{\max} = 0.0033. \end{aligned} \tag{69}$$

As it has been mentioned in section 6, the first conditions which are considered from the stability of the designed SMO point of view are (47). Therefore, taking into account the calculated bounding and Lipschitz constants (69), the 'sliding' gain L^{SMO} and the first term of the 'proportional' gain K_1^{SMO} must meet the following inequalities:

$$L^{\mathrm{SMO}} > 0.0033 + 0.0921 = 0.0954,\ K_1^{\mathrm{SMO}} > 0.05. \tag{70}$$

Taking into account (70) the values of the $\boldsymbol{K}^{\mathrm{SMO}}$ can be selected depending on condition (46), whereas the choice of the L^{SMO} is subject to a certain additional criterion. In order to show the influence of the selection of L^{SMO} on the accuracy (performance) of the estimation process, the designed SMO is examined for three following values of 'sliding' gain:

- $L^{\mathrm{SMO}} = 0$ – the SMO is considered as an only high–gain observer without switching term,
- $L^{\mathrm{SMO}} = 0.1$ – the value of the 'sliding' gain is considered as very close to constrain derived in (70),
- $L^{\mathrm{SMO}} = 20$ – the value of the 'sliding' gain is relatively very high in comparison to the constrain (70).

It is worth adding that these values are selected to show how an additional sliding mode tracker is able to make uncertainty rejected. By setting up $L^{\mathrm{SMO}} = 20$ the equivalent control term is established as $\overline{u}_{\mathrm{eq}} = 20$. Hence, the gain $L^{\mathrm{SMO}} = 20$ significantly exceeds the value of one, calculated from the stability condition and does not result in the peaking phenomenon (because its value is not very high and the approximation function is selected properly). Moreover, due to necessity of chattering phenomenon compensation the function (64) is utilised and its parameter is assumed as $\varepsilon_{\mathrm{sgn}} = 0.01$ (see remark 7).

Next, the global boundedness of the estimation error is investigated. For $L_{\tilde{\boldsymbol{\psi}}} = 0.3323$ the condition (47) insists to select $\boldsymbol{K}^{\mathrm{SMO}}$ which provide to obtain $\lambda_{\max}\left(\boldsymbol{P}_1\right) < 1.5047$. For instance selecting the 'proportional' gain as $\boldsymbol{K}^{\mathrm{SMO}} = \begin{bmatrix} 2 & 2 \end{bmatrix}^{\mathrm{T}}$ this condition holds with $\lambda_{\max}\left(\boldsymbol{P}_1\right) = 1.504$ (to see, how choice of the $\boldsymbol{K}^{\mathrm{SMO}}$ influences on the maximal eigenvalue of Lyapunov matrix check appendix B). For selected $\boldsymbol{K}^{\mathrm{SMO}}$ and $L^{\mathrm{SMO}} = 20$ and also calculated bounding and Lipschitz constants (69), in reaching phase the norm of the estimation error cannot be bigger that $||\tilde{\boldsymbol{\varepsilon}}(t)|| < 433.9817$.

Finally, for the above–mentioned gains $\boldsymbol{K}^{\mathrm{SMO}}$ and L^{SMO} the global asymptotic stability of the designed SMO is ensured by (63). In this work, the analytical solution of (63) is not delivered, hence it is validated in the simulation way.

7.2.2. Estimation results

The estimation results have been obtained assuming the same as in the comparison study (section 7.1) initial conditions for the considered system. Whereas the following initial conditions have been used for the estimating state variables $\hat{\boldsymbol{x}}(0) = \begin{bmatrix}1.2 & 0.7\end{bmatrix}^{\mathrm{T}}$. The trajectories of the state variables (from the cognitive model) and their estimates (from the devised SMO (37)) are presented in Figs. 7 and 8. Four trajectories are shown in each figure: the original state trajectory from the cognitive model and three trajectories of estimates for different values of L^{SMO}.

Analysing the trajectories presented in Figs. 7 and 8, it can be concluded that for the bigger values of L^{SMO}, the performance of estimation is undoubtedly increasing. If $L^{\mathrm{SMO}} = 0$ the SMO dynamics tend is tracking not the original trajectory of the cognitive model but the trajectory associated with the utility model related to the simplified kinetics function. The estimation accuracy for the first state variable is very high practically from the beginning of the simulation, and for the second one, this accuracy is satisfactory after about $t = 100\,[h]$. For more clear presentation the trajectories of absolute values of particular estimation errors, which confirm the above observations are shown in Figs. 9 and 10. Thus, for $L^{\mathrm{SMO}} = 20$, the trajectories of the estimates practically coincide with those of the state variables (dashed red and solid blue lines in Figs. 7 and 8), which yields practically zero estimation errors.

In turn, the behaviour of the original and reconstructed kinetics function by applying formula (26) is given in Fig. 11. Regarding trajectories in Fig. 11, it can be noticed that for the biggest L^{SMO} tracking of the unknown kinetics function is suitable. The comparison of dynamical behaviour presented in Figs. 4, 5 and 6 shows that the additive sliding mode term is able to track the uncertainty and compensate mismatch between the simplified and real dynamics. This, therefore, confirms the robustness and stability of the generated estimates, which have been proven in section 6.

In order to highlight this property and performance of devised SMO in Figs. 12 and 13 the trajectories of state variables and their estimates for different values of L^{SMO} for a wide range of substrate concentration where, e.g., the inhibition cannot be neglected are presented. The obtained results confirm the previous observations, which is further illustrated by the trajectories of estimation errors presented in Figs.14 and 15.

Moreover, in order to show the robustness of the devised SMO, the following analysis is established. For five vastly different initial conditions of the observer $\hat{\boldsymbol{x}}(0)$, constant $\boldsymbol{x}(0)$, and constant gains $\boldsymbol{K}^{\mathrm{SMO}}$ and L^{SMO}, and identical to previous experiments $D(t)$, the simulations have been performed in the face of different behaviour of unknown input $\Delta(\boldsymbol{x}(t), t)$. Taking into account, that the behaviour of $\Delta(\boldsymbol{x}(t), t)$ is dependent on state variables (what has been emphasised in (25)), starting from distinct initial conditions is highly related to the different behaviour of the unknown input. The obtained estimation error trajectories, at the beginning phase, are shown in Figs. 16 and 17. By analysing Figs. 16 and 17 it is easy to notice the convergence of the estimation error trajectories to zero, which confirms the robustness of the devised SMO.

To conclude, as it has been noticed in section 7.2.1, due to the compensation of uncertainty impact on the esti-

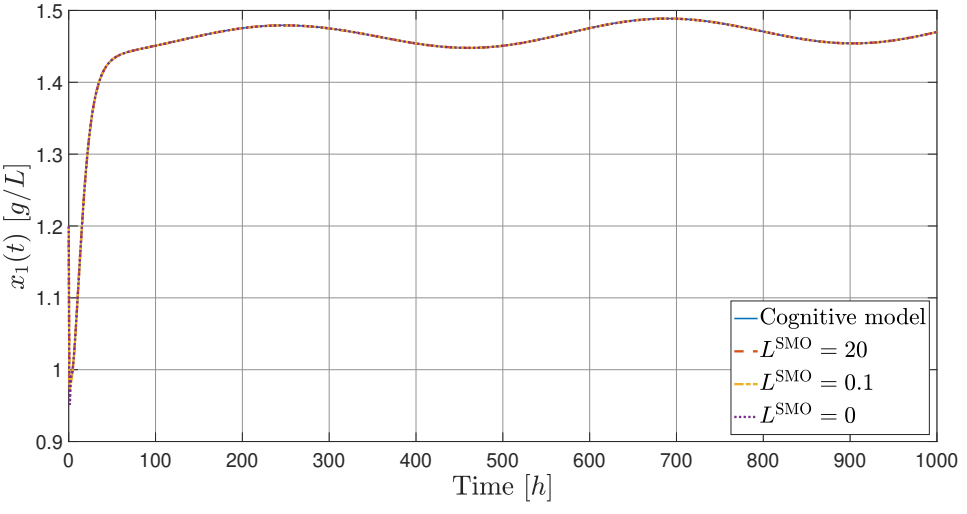

Figure 7: Trajectories of the state variable $x_1(t)$ and its estimates for three values of L^{SMO}.

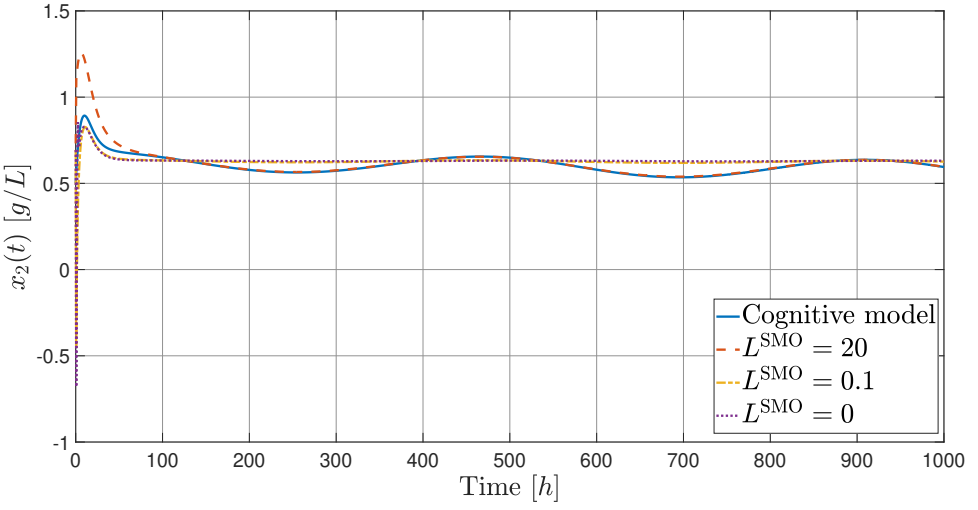

Figure 8: Trajectories of the state variable $x_2(t)$ and its estimates for three values of L^{SMO}.

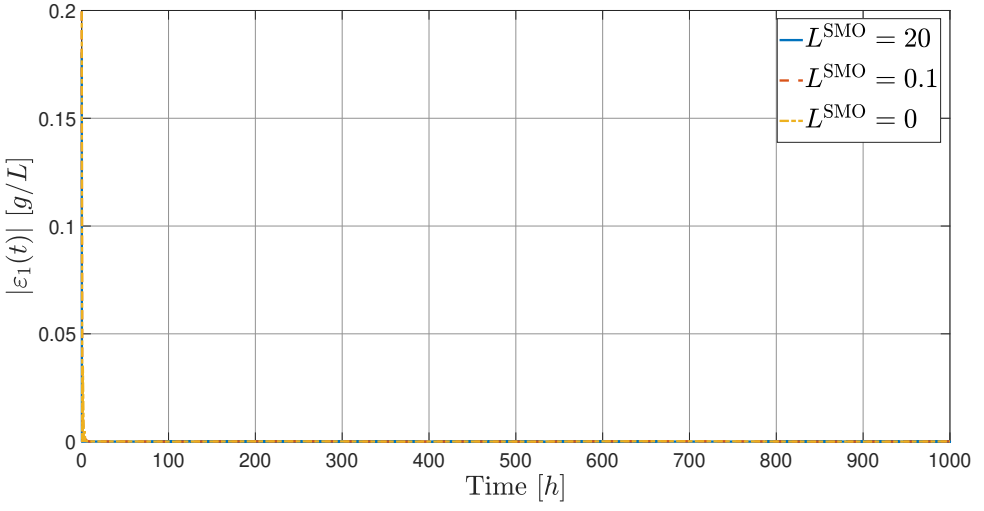

Figure 9: Trajectories of the absolute values of estimation error $\varepsilon_1(t)$ for three values of L^{SMO}.

mation the sliding mode term is crucial. This SMO component is responsible for the rejection of the parametric and unstructured uncertainty or compensation of external, unknown disturbances. In turn, the proportional gain provides identical action as in the classical Luenberger observer, i.e. asymptotic convergence of state estimates to their originals by properly selected gains matrix.

8. Conclusions

In this paper, the problem of state estimation for a certain class of non-linear uncertain dynamical systems has been investigated. In particular, the sliding mode observer has been devised to produce the stable and robust estimates of the state variables in the presence of the parametric and unstructured uncertainty. Hence, the proposed observer is able to reject not only the negative impact of time–varying parameters, but also cope with the uncertainty introduced by unmodelled dynamics. The stability and robustness of the designed sliding mode observer have been rigorously proved. For the observer synthesis purposes, the issues of deriving the correct utility model have been widely discussed. The

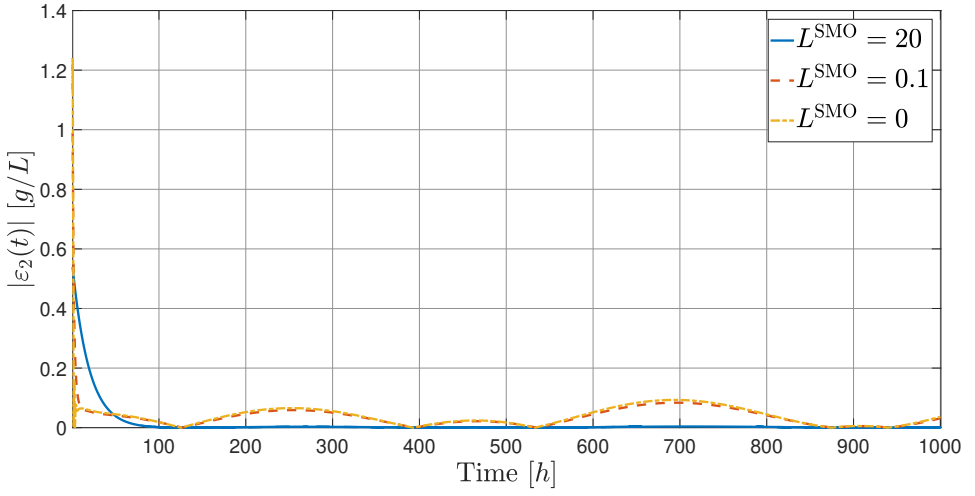

Figure 10: Trajectories of the absolute values of estimation error $\varepsilon_2(t)$ for three values of L^{SMO}.

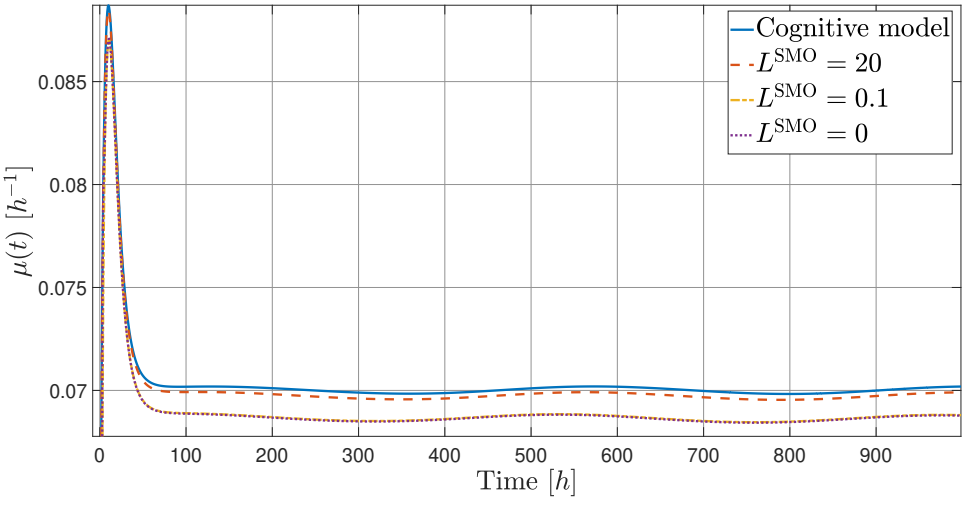

Figure 11: Trajectory of $\mu_{(\cdot)}(t)$ from the cognitive model and its reconstructions for three values of L^{SMO}.

proposed approach is based on treating unknown kinetics function as an external input to the considered system. Thus, the new simplified kinetics function has been given to fulfil observability rank condition and ensuring good mapping of reality. Moreover, the analysis of the influence the observer 'proportional' and 'sliding' gains on the eigenvalues of the Lyapunov matrix as well as the accuracy (performance) of estimation results has been presented. The designed sliding mode observer has been applied to the model of a continuous stirred tank reactor with the microbial growth reaction and their mortality with the aggregated substrate and biomass concentrations. The entire system has been implemented in Matlab/Simulink environment and obtained results yield satisfying performance of the generated estimates.

Future research may focus on extending the proposed methodology to MIMO systems. Furthermore, the idea of simplifying the kinetics function can be used in systems whose dynamics involve concentrations of more than one substrate.

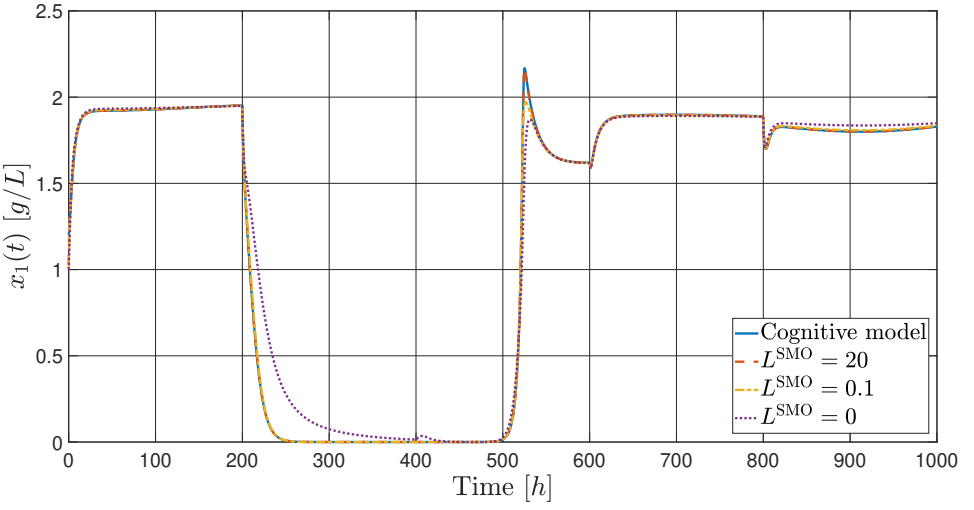

Figure 12: Trajectories of the state variable $x_1(t)$ and its estimates for three values of L^{SMO} for a wide range of substrate concentration.

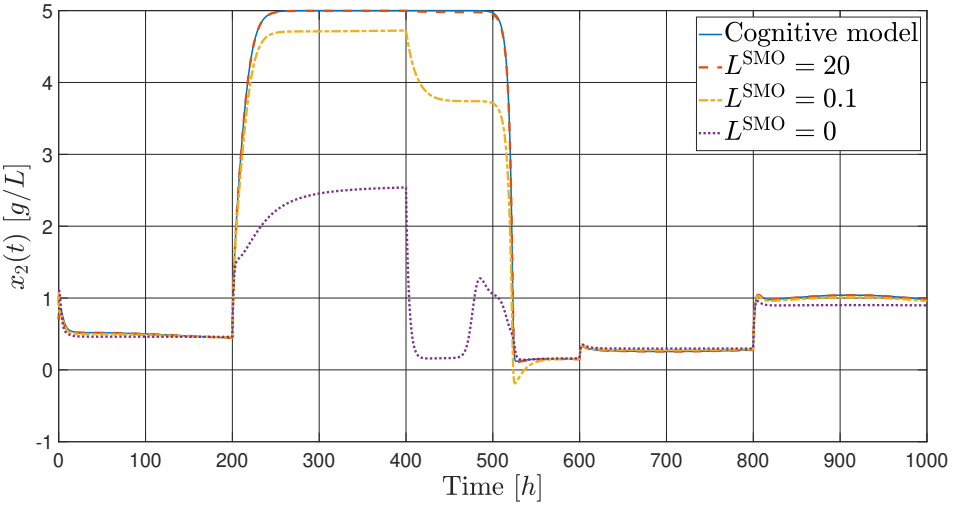

Figure 13: Trajectories of the state variable $x_2(t)$ and its estimates for three values of L^{SMO} for a wide range of substrate concentration.

Acknowledgements

Financial support of these studies from Gdańsk University of Technology by the DEC-2/2020/IDUB/I.3.3 grant under the Argentum Triggering Research Grants - EIRU program is gratefully acknowledged.

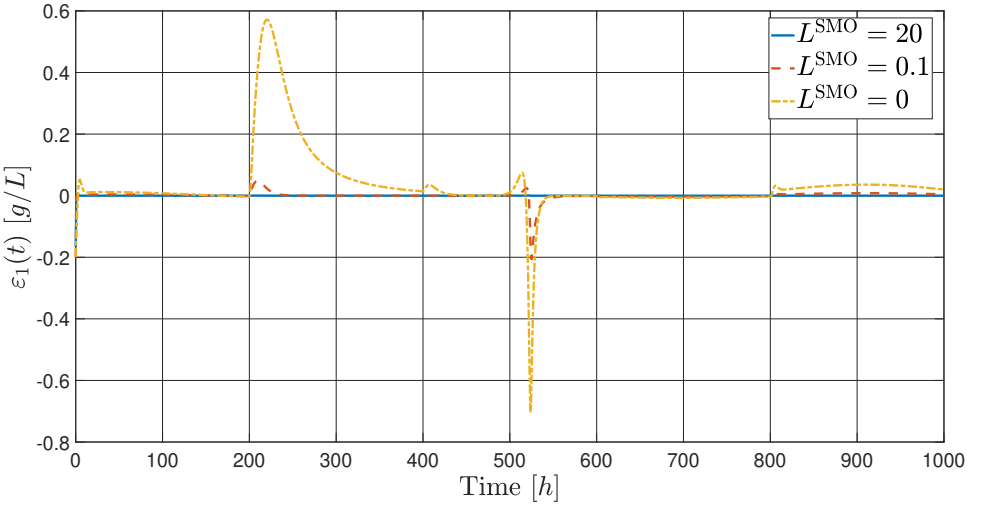

Figure 14: Trajectories of estimation error $\varepsilon_1(t)$ for a wide range of substrate concentration.

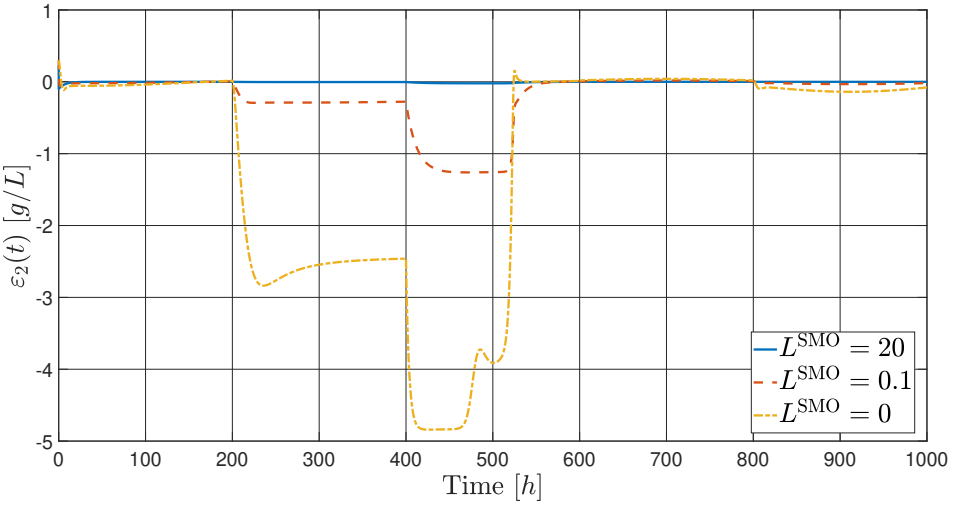

Figure 15: Trajectories of estimation error $\varepsilon_2(t)$ for a wide range of substrate concentration.

A. Discussion on observability

As it has been mentioned above, in order to make state (coordinates) non-linear transformation it is necessary to fulfil two particular conditions. The first of them is associated with a injectivity of transformation whereas the second is associated with the non–singularity of the Jacobi matrix. For the considered utility model of a bioreactor, the kinetics function has been assumed as time–invariant Monod term (21). In general, the calculation of inverse state transformation always involves solving the set of equations. The solution of this set has to be unique. In the considered example the transformation from (27) to (28) is based on solving two algebraic equations with respect to $\boldsymbol{x}(t)$. In comparison to the first equation (it is always identity), the second one needs some more calculation, what for (21) Monod kinetics function is shown below:

$$\tilde{x}_2(t) = \frac{t_1(t)}{t_2(t)}\tilde{x}_1(t) - \beta_{\mathrm{m}}\tilde{x}_1(t),$$

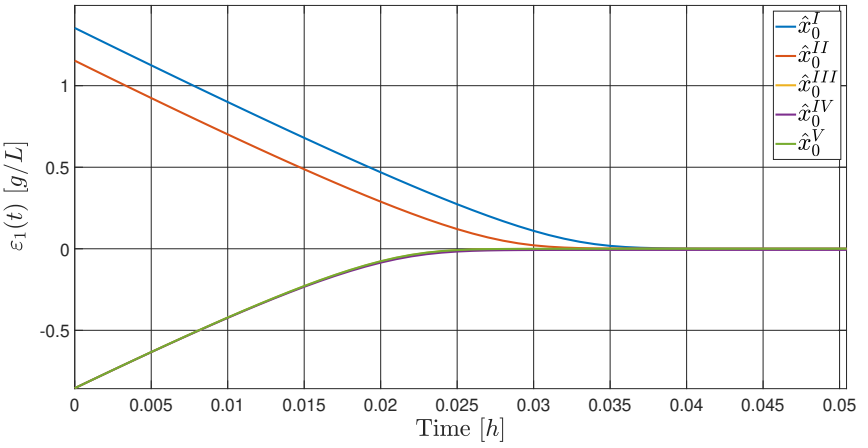

Figure 16: Trajectories of estimation error $\varepsilon_1(t)$ for five different initial conditions.

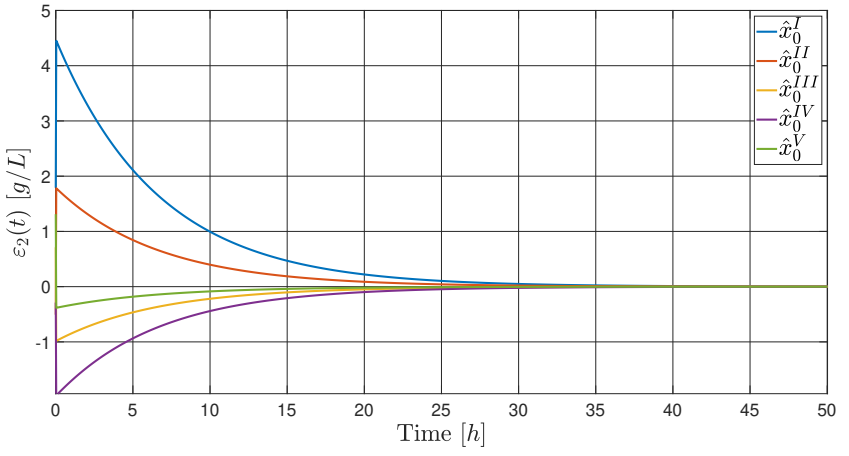

Figure 17: Trajectories of estimation error $\varepsilon_2(t)$ for five different initial conditions.

$$
\begin{aligned}
&t_2(t)\tilde{x}_2(t) = t_1(t)\tilde{x}_1(t) - t_2(t)\beta_{\mathrm{m}}\tilde{x}_1(t),\\
&K_{\mathrm{s}}^0\tilde{x}_2(t) + x_2(t)\tilde{x}_2(t) = t_1(t)\tilde{x}_1(t) - t_4\tilde{x}_1(t) - t_5(t)\tilde{x}_1(t),\\
&x_2(t)\left(\tilde{x}_2(t) + \beta_{\mathrm{m}}\tilde{x}_1(t) - \mu_{\max}^0\tilde{x}_1(t)\right) = K_{\mathrm{s}}^0\left(\tilde{x}_2(t) + \beta_{\mathrm{m}}\tilde{x}_1(t)\right),
\end{aligned}
$$

$$
x_2(t) = \frac{-K_{\mathrm{s}}^0(\tilde{x}_2(t) + \beta_{\mathrm{m}}\tilde{x}_1(t))}{\tilde{x}_2(t) + \beta_{\mathrm{m}}\tilde{x}_1(t) - \mu_{\max}^0\tilde{x}_1(t)}. \tag{71}
$$

In turn, the adaption of $\mu(t)$ as Haldane $\hat{\mu}_H(t)$ presented in (9) with the time–invariant parameters proceeds to the following calculation of state transformation:

$$
\tilde{\boldsymbol{x}}(t) = \boldsymbol{\Phi}(\boldsymbol{x}(t)) = \begin{bmatrix} x_1(t) \\ \mu_0^0 \dfrac{x_2(t)}{t_2(t) + \dfrac{x_2^2(t)}{K_{\mathrm{i}}^0}} x_1(t) - \beta_{\mathrm{m}} x_1(t) \end{bmatrix}, \tag{72}
$$

where μ_0^0 is an estimate of the time–varying parameter $\mu_0(t)$.

In order to obtain the inverse transformation, it is necessary to perform a similar calculations to (71). Unfortunately, in this case, the derivation is impossible because the following expression occurs:

$$x_2^2(t)\left(\tilde{x}_2(t)\frac{1}{K_{\mathrm{i}}^0}+\beta_{\mathrm{m}}\frac{\tilde{x}_1(t)}{K_{\mathrm{i}}^0}\right)+x_2(t)\left(\tilde{x}_2(t)+\beta_{\mathrm{m}}\tilde{x}_1(t)-\mu_{\max}^0\tilde{x}_1(t)\right)=-\beta_{\mathrm{m}}K_{\mathrm{s}}^0\tilde{x}_1(t)-K_{\mathrm{s}}^0\tilde{x}_2(t). \tag{73}$$

The calculations from (73) show that usage of Haldane function for sliding mode observer synthesis is pointless due to non-injectivity of the transformation caused by $x_2^2(t)$ term. Therefore, it is necessary to use a simpler version of the function $\mu(t)$ like, e.g., Monod component which application does not lead to singularity. If the geometrical approach is applied – by calculation of the Jacobian's determinant – it can be easily shown, that the system's states are not observable when $x_1(t) = 0$ or $x_2(t) = \sqrt{K_{\mathrm{s}}^0 K_{\mathrm{i}}^0}$. The first situation can be induced by initial condition or impact of the input $u(t)$ whereas the second one results from the properties of non-monotone Haldane function. In both cases, the singularity of Jacobi matrix (15) occurs what leads to the indistinguishability of the state trajectories. It is worth adding that similar, but not equivalent remarks, can be found in [38, 68, 69]. In these papers, authors considered a different methodology based on the concept of indistinguishable dynamics, which is strictly different than tools based on differential geometry theory [23, 24, 55] for different biochemical reactor structures. This research showed that the Haldane structure is not useful due to the need for deriving injective mapping, what reason from the existence of 'bad inputs' (considered cases have shown that control input $u(t)$ could make states indistinguishable when the singular point is reached) which make two states indistinguishable. It should be noticed that there are also other approaches to overcome the system unobservability in the literature. For example, the methodology based on robust control in partially observable dynamics, which is premised on the utilisation of set-valued, interval observers is presented in [70]. The state observers presented in that approach cope with the problem of uncertain kinetics by assessing unknown part of dynamics by upper and lower estimate, which can be monotone or non-monotone function. In turn, the approach based on uniform exponential observers can be found in [71]. These observers are based on the embedding of original unobservable dynamics to new, extended manifold [72]. In this paper, as it has been mentioned above, the methodology based on analysis of the state observability and detectability of unknown inputs is used. By performing a proper modification of the system's model structure, the unobservable part is 'pushed' into unknown input whereas the dynamics become observable.

B. Analysis of impact of gain matrix values on eigenvalues of the Lyapunov matrix

The matrices $\boldsymbol{A}$, $\boldsymbol{C}$ and $\boldsymbol{K}^{\mathrm{SMO}}$ of the considered system are defined in (36), therefore the dynamics of the linear part of SMO in the new coordinates is given by:

$$\boldsymbol{A}_{\boldsymbol{K}^{\mathrm{SMO}}}=\boldsymbol{A}-\boldsymbol{K}^{\mathrm{SMO}}\boldsymbol{C}=\begin{bmatrix}-K_1^{\mathrm{SMO}} & 1\\ -K_2^{\mathrm{SMO}} & 0\end{bmatrix}. \tag{74}$$

In the context of the stability conditions, the crucial meaning has the investigation of the possibility of changing the maximum eigenvalue – $\lambda_{\max}\left(\boldsymbol{\mathcal{P}}_{(\cdot)}\right)$. Therefore, knowing the form of equation (42) it is possible to research the problem of influencing the particular values of $\boldsymbol{K}^{\mathrm{SMO}}$ on $\boldsymbol{\mathcal{P}}_{(\cdot)}$. Substituting (74) to (42), with assumption that $\boldsymbol{\mathcal{Q}}_{(\cdot)}$ is the identity matrix of dimension 2×2, the equation which might be used to make mentioned investigation is derived as follows:

$$\begin{aligned}
-\begin{bmatrix}1 & 0\\ 0 & 1\end{bmatrix} &= \begin{bmatrix}-K_1^{\mathrm{SMO}} & -K_2^{\mathrm{SMO}}\\ 1 & 0\end{bmatrix}\begin{bmatrix}p_1 & p_2\\ p_2 & p_3\end{bmatrix}+\begin{bmatrix}p_1 & p_2\\ p_2 & p_3\end{bmatrix}\begin{bmatrix}-K_1^{\mathrm{SMO}} & 1\\ -K_2^{\mathrm{SMO}} & 0\end{bmatrix},\\
-\begin{bmatrix}1 & 0\\ 0 & 1\end{bmatrix} &= \begin{bmatrix}-K_1^{\mathrm{SMO}}p_1-K_2^{\mathrm{SMO}}p_2 & -K_1^{\mathrm{SMO}}p_2-K_2^{\mathrm{SMO}}p_3\\ p_1 & p_2\end{bmatrix}+\begin{bmatrix}-K_1^{\mathrm{SMO}}p_1-K_2^{\mathrm{SMO}}p_2 & p_1\\ -K_1^{\mathrm{SMO}}p_2-K_2^{\mathrm{SMO}}p_3 & p_2\end{bmatrix}.
\end{aligned} \tag{75}$$

Owing to (75) it is easy to show that:

$$\begin{cases}1 &= -2p_2\\ 0 &= p_1-\left(K_1^{\mathrm{SMO}}p_2+K_2^{\mathrm{SMO}}p_3\right),\\ 1 &= 2\left(K_1^{\mathrm{SMO}}p_1+K_2^{\mathrm{SMO}}p_2\right)\end{cases} \tag{76}$$

and the solution of (76) is as follows:

$$p_1 = \frac{1 + K_2^{\mathrm{SMO}}}{2K_1^{\mathrm{SMO}}},\ p_2 = -0.5,\ p_3 = \frac{K_1^{\mathrm{SMO}^2} + K_2^{\mathrm{SMO}} + 1}{2K_1^{\mathrm{SMO}} K_2^{\mathrm{SMO}}}. \tag{77}$$

In turn, the calculated eigenvalues of $\boldsymbol{\mathcal{P}}_{(\cdot)}$ are as follows:

$$\lambda_1^{\mathrm{test}} = \frac{1}{2}\left[p_1 + p_3 - \sqrt{\delta^{\mathrm{test}}}\right],\ \lambda_2^{\mathrm{test}} = \frac{1}{2}\left[p_1 + p_3 + \sqrt{\delta^{\mathrm{test}}}\right], \tag{78}$$

where $\delta^{\mathrm{test}} \in \mathbb{R}_+$ is the discriminant of quadratic polynomial to $\delta^{\mathrm{test}} = p_1^2 + 4p_2^2 + p_3^2 - 2p_1p_3$, which must be always positive, due to symmetry of the real matrix $\boldsymbol{\mathcal{P}}_{(\cdot)}$ [61].

Combining (77) and (78) the eigenvalues can be written as:

$$\begin{aligned}
\lambda_1^{\mathrm{test}} &= k_\lambda\left[K_1^{\mathrm{SMO}^2} + K_2^{\mathrm{SMO}^2} + 2K_2^{\mathrm{SMO}}\right] + k_\lambda\left[1 - \mathrm{sgn}\left(K_1^{\mathrm{SMO}}\right)\mathrm{sgn}\left(K_2^{\mathrm{SMO}}\right)\sqrt{\Delta^{\mathrm{test}}}\right], \\
\lambda_2^{\mathrm{test}} &= k_\lambda\left[K_1^{\mathrm{SMO}^2} + K_2^{\mathrm{SMO}^2} + 2K_2^{\mathrm{SMO}}\right] + k_\lambda\left[1 + \mathrm{sgn}\left(K_1^{\mathrm{SMO}}\right)\mathrm{sgn}\left(K_2^{\mathrm{SMO}}\right)\sqrt{\Delta^{\mathrm{test}}}\right],
\end{aligned} \tag{79}$$

where: $k_\lambda = \dfrac{1}{4K_1^{\mathrm{SMO}}K_2^{\mathrm{SMO}}}$, and

$$\Delta^{\mathrm{test}} = K_1^{\mathrm{SMO}^4} + K_2^{\mathrm{SMO}^4} + 2K_1^{\mathrm{SMO}^2}K_2^{\mathrm{SMO}^2} + 2K_1^{\mathrm{SMO}^2} - 2K_2^{\mathrm{SMO}^2} + 1. \tag{80}$$

Taking into account, that gain vector $\boldsymbol{K}^{\mathrm{SMO}}$ (36) is by assumption always positive, the 'signum' expression from (79) must be always equal to one. Finally, $\lambda_{\max}\left(\boldsymbol{\mathcal{P}}_{(\cdot)}\right)$ yields:

$$\lambda_{\max}\left(\boldsymbol{\mathcal{P}}_{(\cdot)}\right) = \max\left\{\lambda_1^{\mathrm{test}}\left(K_1^{\mathrm{SMO}}, K_2^{\mathrm{SMO}}\right), \lambda_2^{\mathrm{test}}\left(K_1^{\mathrm{SMO}}, K_2^{\mathrm{SMO}}\right)\right\} :\ K_1^{\mathrm{SMO}}, K_2^{\mathrm{SMO}} \in \mathbb{R}_+. \tag{81}$$

Therefore, the formulae (79) – (81) can be used to derive maximal eigenvalue of Lyapunov matrix for the two–dimensional considered system. It is worth adding that the derived formulae (79) – (81) must belong to $\mathbb{R}$ field. Hence, the main idea of performed research basing on calculating the biggest eigenvalue for each particular value of assumed matrix $\boldsymbol{K}^{\mathrm{SMO}}$. In particular, assuming that values of both gains may varying in the interval $\langle 0.1\ ;\ 10\rangle$ with resolution equals to 0.1, it has been checked, what is the value of $\lambda_{\max}\left(\boldsymbol{\mathcal{P}}_{(\cdot)}\right)$ for the particular values of K_1^{SMO} and K_2^{SMO}. The obtained results are shown in Fig. 18. As it can be noticed in Fig. 18 the simultaneous increasing values of both gains K_1^{SMO} and K_2^{SMO} causes reducing value of $\lambda_{\max}\left(\boldsymbol{\mathcal{P}}_{(\cdot)}\right)$. In turn, if either both values of gains are near null or one of them is significantly bigger than the other, the value of $\lambda_{\max}\left(\boldsymbol{\mathcal{P}}_{(\cdot)}\right)$ significantly increasing. Another important remark

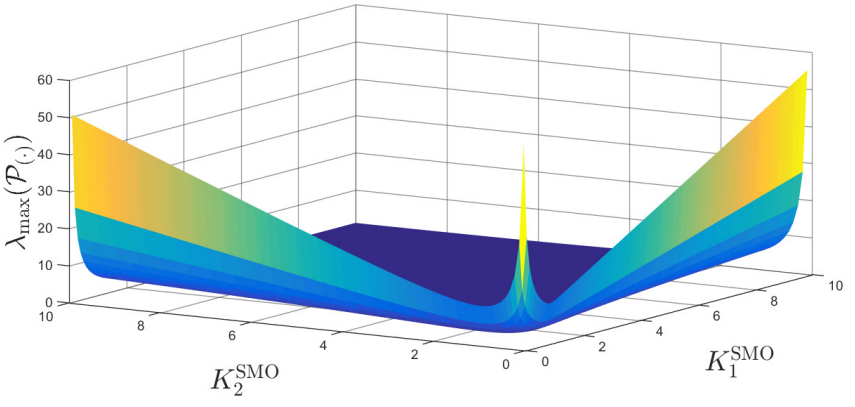

Figure 18: The relation between values of $\lambda_{\max}\left(\boldsymbol{\mathcal{P}}_{(\cdot)}\right)$ and $\boldsymbol{K}^{\mathrm{SMO}}$.

is associated with the next test when very high values have been set in the gains matrix. It can be observed that when values of $K_1^{\mathrm{SMO}},\ K_2^{\mathrm{SMO}} \to \infty$, the maximum eigenvalue $\lambda_{\max}\left(\boldsymbol{\mathcal{P}}_{(\cdot)}\right) \to 1$. This clearly shows that the structure of the SMO in the new coordinates enforces some inherent limitations on the possibility of changes $\lambda_{\max}\left(\boldsymbol{\mathcal{P}}_{(\cdot)}\right)$. It is worth adding that despite the presented considerations has included only the two–dimensional system, the used methodology of SMO synthesis always provide to the same 'new' general form of the system dynamics. The consequence is that for each particular system the value changing range of $\lambda_{\max}\left(\boldsymbol{\mathcal{P}}_{(\cdot)}\right)$ is very limited and homogeneous. Hence, for systems whose bounding constants are too 'large', it is not possible to prove global limitation and global asymptotic stability of the estimation error according to the formulae presented in the publications [25, 36, 39, 40].

C. Methodology for determining the bounding and Lipschitz constants

Due to the fact that the presented SMO synthesis requires determining the Lipschitz constants as well as the bounding constants the certain methodological aspects of their computations should be explained. It is well–known that the analytical calculations of global or local Lipschitz constants are distinctly compound, the authors proposed to employ an alternative approach based on a combination of functional analysis and optimisation methods. The certain methodological aspects of this approach can be found also in, e.g., [56, 57].

Computation of Lipschitz constant

Taking the n_{Lip}–dimensional function $\boldsymbol{F}^{\mathrm{Lip}}$ class $C^{\infty}\left(\boldsymbol{X}_{\mathrm{m_{Lip}}}^{\mathrm{Lip}}\right)$, where $\boldsymbol{X}_{\mathrm{m_{Lip}}}^{\mathrm{Lip}} \subset \mathbb{R}^{\mathrm{m_{Lip}}}$ is a convex (invariant) set considering as $\mathrm{m_{Lip}}$–dimensional hyper–cube, which arguments x^{Lip} are spanning m_{Lip}–dimensional space (e.g. time–varying variables such as the state variables or inputs). Using the functional analysis approach, the optimal Lipschitz constant (L_{Lip}^{*}) can be computed by calculation of infinity norm of Jacobi matrix [43]:

$$\left\| \frac{\partial \boldsymbol{F}^{\mathrm{Lip}}}{\partial \boldsymbol{x}^{\mathrm{Lip}}} \right\|_{\infty} \leq L_{\mathrm{Lip}}^{*},\ L_{\mathrm{Lip}}^{*} \in \mathbb{R}_{+}, \tag{82}$$

where $||\cdot||_{\infty}$ denotes an infinity norm of matrix [43, 62].

For the determination of Lipschitz constants associated with the proposed SMO observer synthesis, assuming *a priori* known bounds on the state vector $\boldsymbol{x}(t)$ the following approach can be used. This approach is based on solving an appropriate optimisation task with respect to objective function (82). The optimisation task is formulated as follows:

$$\left\| \frac{\partial \boldsymbol{F}^{\mathrm{Lip}}}{\partial \boldsymbol{x}^{\mathrm{Lip}}} \right\|_{\infty} = \max\left\{ \mathcal{S} = \left\{ S_{j_{\mathrm{Lip}}} \right\}_{j_{\mathrm{Lip}}=1}^{n_{\mathrm{Lip}}} \right\} \leq L_{\mathrm{Lip}}, \tag{83}$$

$$S_{j_{\mathrm{Lip}}} = \max\left\{ \left\| \nabla_{\boldsymbol{x}^{\mathrm{Lip}}} \boldsymbol{F}^{\mathrm{Lip}} \right\|_{1} = \sum_{i_{\mathrm{Lip}}=1}^{n_{\mathrm{Lip}}} \left| \frac{\partial F_{j_{\mathrm{Lip}}}^{\mathrm{Lip}}}{\partial x_{i_{\mathrm{Lip}}}^{\mathrm{Lip}}} \right| :\ \boldsymbol{x}^{\mathrm{Lip}} \in \boldsymbol{X}_{\mathrm{m_{Lip}}}^{\mathrm{Lip}} \right\},$$

$$j_{\mathrm{Lip}} = \overline{1, n_{\mathrm{Lip}}},\ i_{\mathrm{Lip}} = \overline{1, m_{\mathrm{Lip}}}.$$

where $||\cdot||_1$ is a vector norm [43, 62].

Hence, calculating the maximal value from the set $\mathcal{S}$, the Lipschitz constant, which covers with (82), is established. Taking into account that for each of $S_{j_{\mathrm{Lip}}}$, the maximal value of its $||\cdot||_1$ must be calculated, in general, the problem of Lipschitz constant computation can be considered as a non-linear convex optimisation task.

Computation of bounding constant

In general, n_{bound}–dimensional function $\boldsymbol{f}^{\mathrm{bound}}$ class $C^{\infty}\left(\boldsymbol{X}_{\mathrm{m_{bound}}}^{\mathrm{bound}}\right)$, which arguments x^{bound} are spanning m_{bound}–dimensional space is considered. The computation of bounding constant $C_{\mathrm{bound}} \in \mathbb{R}_{+}$ is similar to the calculation of Lipschitz constant (83). Therefore, assuming that $\boldsymbol{X}_{\mathrm{m_{bound}}}^{\mathrm{bound}}$ has the same meaning as $\boldsymbol{X}_{\mathrm{m_{Lip}}}^{\mathrm{Lip}}$, the optimisation task can be formulated as follows:

$$\left\| \boldsymbol{f}^{\mathrm{bound}} \right\|_{\infty} = \max\left\{ \left\| \boldsymbol{f}^{\mathrm{bound}} \right\|_{2} :\ \boldsymbol{x}^{\mathrm{bound}} \in \boldsymbol{X}_{\mathrm{m_{bound}}}^{\mathrm{bound}} \right\} \leq C_{\mathrm{bound}}. \tag{84}$$

Hence, the optimal value of bounding constant is established by calculating $||\cdot||_\infty$ norm which is considered as maximising a $||\cdot||_2$ norm of function $\boldsymbol{f}^{\text{bound}}$ on the set $\boldsymbol{X}^{\text{bound}}_{\text{m}_{\text{bound}}}$.

References

[1] R. Łangowski and M. A. Brdys. An optimised placement of the hard quality sensors for a robust monitoring of the chlorine concentration in drinking water distribution systems. *Journal of Process Control*, 68:52–63, 2018. doi: https://doi.org/10.1016/j.jprocont.2018.04.007.

[2] J. Yu, V. M. Zavala, and M. Anitescu. A scalable design of experiments framework for optimal sensor placement. *Journal of Process Control*, 67:44–55, 2018. doi: https://doi.org/10.1016/j.jprocont.2017.03.011.

[3] R. Ortega, A. Bobtsov, D. Dochain, and N. Nikolaev. State observers for reaction systems with improved convergence rates. *J Process Control*, 83:53–62, 2019. doi: https://doi.org/10.1016/j.jprocont.2019.08.003.

[4] G. Besancon. *Nonlinear observers and applications*. Springer-Verlag, Berlin, Germany, 2007.

[5] D. G. Luenberger. An introduction to observers. *IEEE Transactions on Automatic Control*, 16:596–602, 1971. doi: 10.1109/TAC.1971.1099826.

[6] R. E. Kalman. A new approach to linear filtering and prediction problems. *Transactions of the ASME - Journal of Basic Engineering*, 82: 35–45, 1960. doi: 10.1115/1.3662552.

[7] R. Łangowski and M. A. Brdys. An interval estimator for chlorine monitoring in drinking water distribution systems under uncertain system dynamics, inputs and chlorine concentration measurement errors. *International Journal of Applied Mathematics and Computer Science*, 27 (2):309–322, 2017. doi: 10.1515/amcs-2017-0022.

[8] D. Efimov and T. Raïssi. Design of interval observers for uncertain dynamical systems. *Automation and Remote Control*, 77(2):191–225, 2016. doi: 10.1134/S0005117916020016.

[9] J. L. Gouzé, A. Rapaport, and M. Z. Hadj-Sadok. Interval observers for uncertain biological systems. *Ecological Modelling*, 133:45–56, 2000. doi: https://doi.org/10.1016/S0304-3800(00)00279-9.

[10] A. Rapaport and D. Dochain. Interval observers for biochemical processes with uncertain kinetics and inputs. *Mathematical Biosciences*, 193:235–253, 2005. doi: 10.1016/j.mbs.2004.07.004.

[11] M. Farza, K. Busawon, and H. Hammouri. Simple nonlinear observers for on-line estimation of kinetic rates in bioreactors. *Automatica*, 34: 301–318, 1998. doi: https://doi.org/10.1016/S0005-1098(97)00166-0.

[12] H. K. Khalil and L. Praly. High-gain observers in nonlinear feedback control. *International Journal of Robust and Nonlinear Control*, 24: 993–1015, 2013. doi: 10.1002/rnc.3051.

[13] K. C. Veluvolu and Y. C. Soh. *Nonlinear sliding mode state and unknown input estimations*. VDM Verlag Dr. Muller, Saarbrucken, Germany, 2009.

[14] M. Farza, M. M'Saad, T. Ménard, A. Ltaief, and T. Maatoug. Adaptive observer design for a class of nonlinear systems. application to speed sensorless induction motor. *Automatica*, 90:239–247, 2018. doi: https://doi.org/10.1016/j.automatica.2017.12.058.

[15] E. Alvaro-Mendoza, J. De León-Morales, and O. Salas-Peña. State and parameter estimation for a class of nonlinear systems based on sliding mode approach. *ISA T*, In Press, 2020. doi: https://doi.org/10.1016/j.isatra.2020.12.018.

[16] T. Boukhobza, M. Djemai, and J.P. Barbot. Implicit triangular observer form dedicated to a sliding mode observer for systems with unknown inputs. *Chemical Engineering Journal*, 5:513–527, 2003. doi: https://doi.org/10.1111/j.1934-6093.2003.tb00169.x.

[17] S. Drakunov and V Utkin. Sliding mode observers. Tutorial. In *Proceedings of the 34th Conference on Decision 81 Control*, pages 3376–3378, 1995. doi: 10.1109/CDC.1995.479009.

[18] C. Edwards, S. Spurgeon, and R. J. Patton. Sliding mode observers for fault detection and isolation. *Automatica*, 36:541–553, 2000. doi: https://doi.org/10.1016/S0005-1098(99)00177-6.

[19] L. Fridman, J. Moreno, and R. Iriarte. *Sliding Modes after the First Decade of the 21st Century*. Springer-Verlag, Berlin, Germany, 2011.

[20] Y. Shtessel, C. Edwards, L. Fridman, and A. Levant. *Sliding mode control and observation*. Birkhäuser, New York, NY, US, 2014.

[21] J.J. Slotine, J.K. Hendrick, and E.A. Misawa. On sliding observers for nonlinear systems. In *1986 American Control Conference*, pages –, 1986. doi: 10.23919/ACC.1986.4789217.

[22] K. Hfaïedh, K. Dahech, and T. Damak. Observer-based output feedback integral terminal sliding mode control for nonlinear systems: multi-model approach. *International Journal of Modelling, Identification and Control*, 34(3):225–234, 2020. doi: https://doi.org/10.1504/IJMIC.2020.111618.

[23] J. Moreno and D. Dochain. Global observability and detectability analysis of uncertain reaction systems and observer design. *International Journal of Control*, 81:1062–1070, 2008. doi: 10.1080/00207170701636534.

[24] J. Moreno, E. Rocha-Cozatl, and A. Vande Wouwer. Observability/detectability analysis for nonlinear systems with unknown inputs - application to biochemical processes. In *Preprints of the 2012 20th Mediterranean Conference on Control & Automation (MED)*, pages 2445–2450, 2012. doi: 10.1109/MED.2012.6265630.

[25] K. C. Veluvolu and Y. C. Soh. Nonlinear sliding mode observers for state and unknown input estimations. In *Proceedings of the 46th IEEE Conference on Decision and Control*, pages 4347–4352, 2007. doi: 10.1109/CDC.2007.4434592.

[26] M. Reichhartinger, S. K. Spurgeon, and M. Weyrer. Design of an unknown input observer to enhance driver experience of electric power steering systems. In *2016 European Control Conference (ECC)*, pages –, 2016. doi: 10.1109/ECC.2016.7810297.

[27] R. Seliger and P. M. Frank. Fault-diagnosis by disturbance decoupled nonlinear observers. In *Proceedings of the 30th IEEE Conference on Decision and Control*, pages –, 1991. doi: 10.1109/CDC.1991.261547.

[28] Y. Xiong and M. Saif. Sliding mode observer for nonlinear uncertain systems. *IEEE Transactions on Automatic Control*, 46:2012–2017, 2001. doi: 10.1109/9.975511.

[29] X. Wu, Y. Zhao, and K. Xu. Nonlinear disturbance observer based sliding mode control for a benchmark system with uncertain disturbances.

ISA Transactions, In Press, 2020. doi: https://doi.org/10.1016/j.isatra.2020.10.032.
[30] J. Chang, J. Cieslak, Z. Guo, and D. Henry. On the synthesis of a sliding-mode-observer-based adaptive fault-tolerant flight control scheme. *ISA Transactions*, In Press, 2020. doi: https://doi.org/10.1016/j.isatra.2020.10.061.
[31] H. De Battista, J. Picó, F. Garelli, and J. L. Navarro. Reaction rate reconstruction from biomass concentration measurement in bioreactors using modified second-order sliding mode algorithms. *Bioprocess and Biosystems Engineering*, 35:1615–1625, 2012. doi: https://doi.org/10.1007/s00449-012-0752-y.
[32] J. Gonzalez, G. Fernandez, R. Aguilar, M. Barron, and J. Alvares-Ramirez. Sliding mode observer-based control for a class of bioreactors. *Chemical Engineering Journal*, 83:25–32, 2001. doi: https://doi.org/10.1016/S1385-8947(00)00177-7.
[33] J. Moreno and J. Alvarez. A bivalued observer for a class of uncertain reactors. *IFAC Proceedings Volumes*, 46:261–266, 2013. doi: https://doi.org/10.3182/20131216-3-IN-2044.00023.
[34] E. Rocha-Cozatl, M. Sbarciog, L. Dewasme, J. Moreno, and A. Vande Wouwer. State and input estimation of an anaerobic digestion reactor using a continuous-discrete unknown input observer. *IFAC-PapersOnLine*, 48:129–134, 2015. doi: https://doi.org/10.1016/j.ifacol.2015.08.169.
[35] A. Vargas, J. Moreno, and A. Vande Wouwer. A weighted variable gain super-twisting observer for the estimation of kinetic rates in biological systems. *Journal of Process Control*, 24:957–965, 2014. doi: https://doi.org/10.1016/j.jprocont.2014.04.018.
[36] K. C. Veluvolu, Y. C. Soh, and W. Cao. Robust observer with sliding mode estimation for nonlinear uncertain systems. *IET Control Theory & Applications*, 1:1533–1540, 2007. doi: 10.1049/iet-cta:20060434.
[37] D. Dochain and P. Vanrolleghem. *Dynamical modelling and estimation in wastewater treatment processes*. IWA Publishing, London, UK, 2001.
[38] J. Moreno and A. Vargas. Nonlinear observer design and observability of an aerobic bioreactor using respirometry. In *1999 European Control Conference (ECC)*, pages –, 1999. doi: 10.23919/ECC.1999.7099523.
[39] K. C. Veluvolu, Y. C. Soh, W. Cao, and Z. Y. Liu. Observer with multiple sliding modes for a class of nonlinear uncertain systems. In *2005 American Control Conference*, pages 2445–2450, 2005. doi: 10.1109/ACC.2005.1470333.
[40] K. C. Veluvolu, M. Defoort, and Y.C. Soh. High-gain observer with sliding mode for nonlinear state estimation and fault reconstruction. *Journal of the Franklin Institute*, 351:1995–2014, 2013. doi: http://dx.doi.org/10.1016/j.jfranklin.2012.12.018.
[41] J. C. Doyle and G. Stein. Robustness with observers. *IEEE Transactions on Automatic Control*, 24:607–611, 1979. doi: 10.1109/TAC.1979.1102095.
[42] A. Isidori. *Nonlinear control systems*. Springer-Verlag London, London, UK, 1995.
[43] H. K. Khalil. *Nonlinear systems, 3rd edition*. Prentice–Hall, Inc., Upper Saddle River, NJ, US, 2002.
[44] G. Bastin, L. Chen, and V. Chotteau. Can we identify biotechnological processes? *IFAC Proceedings Volumes*, 25:83–88, 1992. doi: https://doi.org/10.1016/S1474-6670(17)50330-4.
[45] D. Dochain and M. Perrier. A state observer for (bio)processes with uncertain kinetics. In *Proceedings of the 2002 American Control Conference*, pages 2873–2878, 2002. doi: 10.1109/ACC.2002.1025225.
[46] I. Didi, H. Dib, and B. Cherki. A Luenberger-type observer for the AM2 model. *Journal of Process Control*, 32:117–126, 2015. doi: https://doi.org/10.1016/j.jprocont.2015.04.010.
[47] N. J. Horan. *Biological wastewater treatment systems - theory and operation*. John Wiley & Sons, Chichester, UK, 1990.
[48] G. Bastin and D. Dochain. *On–line estimation and adaptive control of bioreactors*. Elsevier Science Publishers, Amsterdam, Netherlands, 1990.
[49] T. Caraballo, R. Colucci, J. López-de-la Cruz, and A. Rapaport. Study of the chemostat model with non-monotonic growth under random disturbances on the removal rate. *Math Biosci Eng*, 17(6):7480–7501, 2020. doi: 10.3934/mbe.2020382.
[50] J. P. Gauthier and I. A. K. Kupka. Observability and observers for nonlinear systems. *SIAM Journal on Control and Optimization*, 32:975–994, 1994. doi: https://doi.org/10.1137/S0363012991221791.
[51] R. Hermann and A. Krener. Nonlinear controllability and observability. *IEEE Transactions on Automatic Control*, 22:728–740, 1977. doi: 10.1109/TAC.1977.1101601.
[52] V. Utkin. *Sliding modes in control and optimizations*. Springer-Verlag, Berlin, Germany, 1992.
[53] M. Spivak. *A comprehensive introduction to differential geometry. Vol. 1, 3rd Edition*. Publish or Perish, INC., Houston, Texas, US, 1999.
[54] A. J. Krener and A. Isidori. Linearization by output injection and nonlinear observers. *Systems & Control Letters*, 3:47–52, 1983. doi: https://doi.org/10.1016/0167-6911(83)90037-3.
[55] S. Ibarra-Rojas, J. Moreno, and G. Espinosa-Pérez. Global observability analysis of sensorless induction motors. *Automatica*, 40:1079–1085, 2004. doi: https://doi.org/10.1016/j.automatica.2004.01.020.
[56] R. Rajamani. Observers for Lipschitz nonlinear systems. *IEEE Transactions on Automatic Control*, 43:397–401, 1998. doi: 10.1109/9.661604.
[57] G. Phanomchoeng and R. Rajamani. On the difference between bounded Jacobian and Lipschitz observers for nonlinear estimation applications. *Transactions - Canadian Society for Mechanical Engineering*, 41:395–415, 2017. doi: 10.1139/tcsme-2017-0028.
[58] A. Chakrabarty, A. Rundell, S. H. Żak, F. Zhu, and G. T. Buzzard. Unknown input estimation for nonlinear systems using sliding mode observers and smooth window functions. *SIAM Journal on Control and Optimization*, 56(5):3619–3641, 2018. doi: 10.1137/16M1078793.
[59] B. Alenezi, J. Hu, and S. H. Żak. Adaptive unknown input and state observers. In *2019 American Control Conference (ACC)*, pages –, 2019. doi: 10.23919/ACC.2019.8815288.
[60] A. Alessandri. Design of sliding-mode observers and filters for nonlinear dynamic systems. In *Proceedings of the 39th IEEE Conference on Decision and Control*, pages –, 2000. doi: 10.1109/CDC.2000.914194.
[61] S. Boyd, L. El Ghaoui, E. Feron, and B. Venkataramanan. *Linear matrix inequalities in system and control theory*. Society for Industrial and Applied Mathematics, Philadelphia, Pennsylvania, US, 1994.
[62] G. Shilov and G. Chilov. *Elementary functional analysis*. Courier Corporation, Moscow, Russia, 1996.
[63] K. Kalsi, J. Lian, S. Hui, and S. H. Żak. Sliding-mode observers for uncertain systems. In *2009 American Control Conference*, pages

1189–1194, 2009. doi: 10.1109/ACC.2009.5159813.

[64] C. Aboky, G. Sallet, and J.C. Vivalda. Observers for Lipschitz non-linear systems. *International Journal of Control*, 75:204–212, 2002. doi: 10.1080/00207170110107256.

[65] R. Rajamani and Y.M. Cho. Existence and design of observers for nonlinear systems: Relation to distance to unobservability. *International Journal of Control*, 69:717–731, 1998. doi: 10.1080/002071798222640.

[66] H. J. Sussmann and P. V. Kokotovic. The peaking phenomenon and the global stabilization of nonlinear systems. *IEEE Transactions on Automatic Control*, 36:424–440, 1991. doi: 10.1109/9.75101.

[67] A. M Herek, S. W. Su, H. M. Trinh, and Q. P. Ha. Performance of first and second-order sliding mode observers for nonlinear systems. In *Proceedings of the 3rd International Workshop on Artificial Intelligence in Science and Technology*, pages 1–7, 2009. doi: http://hdl.handle.net/10453/11994.

[68] A. Schaum, J. Moreno, and A. Vargas. Global observability and detectability analysis for a class of nonlinear models of biological processes with bad inputs. In *2005 2nd International Conference on Electrical and Electronics Engineering*, pages –, 2005. doi: 10.1109/ICEEE.2005.1529640.

[69] A. Schaum and J. Moreno. Dynamical analysis of global observability properties for a class of biological reactors. In *10th International IFAC Symposium on Computer Applications in Biotechnology*, pages 213–218, 2007. doi: 10.3182/20070604-3-MX-2914.00037.

[70] A. Rapaport and J. Harmand. Robust regulation of a class of partially observed nonlinear continuous bioreactors. *Journal of Process Control*, 12(2):291–302, 2002. doi: https://doi.org/10.1016/S0959-1524(01)00029-4.

[71] A. Rapaport and M. Maloum. Design of exponential observers for nonlinear systems by embedding. *International Journal of Robust and Nonlinear Control*, 14:273–288, 2004. doi: https://doi.org/10.1002/rnc.878.

[72] N. Nijmeijer and A. J. Van der Schaft. *Nonlinear dynamical control systems*. Springer-Verlag, New York, US, 1990.

Mateusz Czyżniewski received the M.Sc. degree (Hons.) in control engineering from the Faculty of Electrical and Control Engineering at the Gdańsk University of Technology in 2019. Since October 2019, he has been a Ph.D. student at the Gdańsk University of Technology in the field of Control Engineering. His research interests involve advanced non-linear control theory, mathematical modelling of dynamical systems, and robust estimation and monitoring methods.

Rafał Łangowski received the M.Sc. and the Ph.D. degrees (Hons.) in control engineering from the Faculty of Electrical and Control Engineering at the Gdańsk University of Technology in 2003 and 2015, respectively. From 2007 to 2014, he held the specialist as well as manager positions at ENERGA, one of the biggest energy enterprises in Poland. Since February 2014, he has been an owner of VIDEN a business in energy and control areas. He provides theoretical and practical experience, especially in front and back office at energy company and operation of the energy market in Poland. From 2016 to 2017, he was a Senior Lecturer with the Department of Control Systems Engineering at the Gdańsk University of Technology. He is currently an Assistant Professor with the Department of Electrical Engineering, Control Systems and Informatics. His research interests involve mathematical modelling and identification, estimation methods, especially state observers, and monitoring of large scale complex systems.